MSc Thesis

Managing freshwater lenses in a Dutch coastal setting;

increasing freshwater availability by aquifer storage and recovery.

Maitri Fischer

Student No. 3592375

November 16, 2012

Programme	MSc. Hydrology, track Environmental Hydrogeology
Supervisors	Esther van Baaren (Deltares)
	Pieter Pauw (Deltares)
	Prof. Dr. Ruud Schotting (Utrecht University)

Abstract

Farmers in the coastal area of Walcheren, Zeeland are faced with issues of salt-water intrusion and summer drought (*Oude Essink et al.*, 2010). These coastal areas are naturally brackish-saline environments due to Holocene marine transgressions (*Stuyfzand and Stuurman*, 1994; *Post et al.*, 2003). Farming in these coastal areas relies on the existence of freshwater lenses that float on top of saline groundwater. These freshwater lenses are much smaller (< 10 m) than what is typically found in the dunes and are the product of the balance between infiltrating rainwater and saline seepage (*Eeman et al.*, 2011; *De Louw et al.*, 2011). This research provides an investigation into the hydrology of the dune area between Oostkapelle and Vrouwenpolder and on the freshwater lenses found on the farmlands. This research comprises a physical investigation of the shallow hydrological system using geophysical methods and a density dependent groundwater flow and solute transport model with the numerical transport code MOCDENS3D.

Electrical conductivity (EC), temperature-EC probe and EM-31 results pinpoint three likely locations of saline seepage. It is advised that the saline water be routed away from the interest area towards the east so as to ensure several ditches remain fresh for aquifer freshwater storage. Continuous vertical electrical sounding measurement transects reveal freshwater lenses of no average between 6 m and 8 m deep. Two proposed measures to increase the availability of freshwater and decrease saline seepage are investigated with the model. Firstly, phreatic aquifer storage and recovery scenarios on two separate farmland plots are investigated. Surplus freshwater during winter is pumped into the subsurface through a horizontal well for recovery and use during times of need as often occurs in summer. Second, a proposed new ditch drainage level scheme is tested to investigate its effects on saline seepage and the shallow subsurface freshwater system.

Results of both aquifer storage and recovery scenarios indicate that an injection of 10000 m^3 of freshwater over six months in winter and an abstraction of 6000 m^3 of water in summer is sustainable over long periods of time and does not cause further salinization of the shallow subsurface. Results of the scenario study for the newly proposed drainage ditch water levels showed that no significant change was observable to the depths of the freshwater lenses on the farmland plots, and there was a marked reduction of seepage and chloride concentrations in the ditches due to the increase in ditch water levels. However it was observed that the size and amount of more diffusive like seepage on the farmland plots increased.

Farmers in the coastal areas of the Netherlands will be increasingly faced with the challenges of summer droughts and saline seepage due to climate change and sea level rise. The findings of this research outlines a low cost and effective way to store water for later use such as in dry summer month and has great potential to help coastal farming and irrigation practices in similar coastal environments.

Contents

List of Tables

List of Figures

1 Introduction

More than half of the world's population lives within 60 km of the shoreline (*U.N.*, 1994). Freshwater availability and access is critical to our survival and the existence of large cities. The issue of salinization of coastal land and freshwater shortages are faced by people in all areas of the world. Large coastal cities often face saline water intrusion and even severe subsidence due to water production for agriculture, households and industry. According to the latest UN-HABITAT report, by 2050, the population of people living in large cities is expected to reach 70%, with a projected global population of around nine billion people (*Eduardo López Moreno*, 2008). Exacerbated by the effects of climate change and sea level rise, coastal populations will have to face ever increasing freshwater challenges to come (*Stuyfzand*, 1993).

Coastal areas of the Netherlands are naturally brackish-saline environments due to Holocene marine transgressions (*Stuyfzand and Stuurman*, 1994; *Post et al.*, 2003; *Post and Abarca*, 2010). The south-western delta of the Netherlands and Belgium, where the Rhine, Meuse and the Scheldt rivers empty into the North Sea, form an elaborate delta with fan-like river patterns, waterways and islands (see figure 1a). In the last millennium, this deltaic area was heavily shaped by human activity like drainage and embankments (*Oude Essink*, 2001). Land subsidence, caused by peat extraction/oxidation and clay compaction (from dewatering) further contributed to the development of low lying areas that became increasingly prone to flooding. The advancement of technology (windmills to mechanical drainage to pumps) and the creation of polders drove ever more land reclamation from the sea and inland lakes. Today, roughly 25% of the Netherlands is below mean sea level (MSL) and many areas suffer high salt loads and saline seepage issues (upward flowing saline groundwater). Salinization of surface and shallow subsurface freshwater can have great consequences on local farming and irrigation practices. Surface water and groundwater can be rendered useless for farming from salt intrusion.

With an expected rise in sea level, hydrological gradients between the sea and low lying areas will increase, resulting in an increase in saltwater intrusion and salt load to shallow subsurface and surface water bodies (*Van der Meij*, 1999; *Oude Essink et al.*, 2010; *De Louw et al.*, 2011). According to the *Veerman* (2008) report, considering subsidence in the Netherlands, local sea level rise by 2100 is expected to be around 0.65 - 1.3 m with respect to the Dutch Ordnance Datum, NAP. *Oude Essink et al.* (2010) showed, with model simulations, that salt loads of seepage into some low lying polders could double from sea level rise by 2100. Saline seepage, summer droughts along with the scarce availability of fresh water is a serious challenge for local farmers in coastal areas of the Netherlands, and with future climate change, problems pertaining to freshwater availability will most likely increase.

On the farmland, drainage ditches are needed to keep the groundwater table artificially low and drain excess water. In areas that lie around MSL, this has resulted in saline seepage. Farming is only made possible due to the physical existence of freshwater lenses which lie (or float) on top of brackish to saline groundwater. These lenses which are typically only several meters to tens of meters thick are created by the equilibrium between buoyancy forces, downward flowing recharge and saline seepage. The few meters of freshwater is all that farmers have to rely on. In summer months, when recharge is low and crops are growing, freshwater lenses contract and what freshwater is left often

becomes contaminated by saline seepage. Farming practices, which often use tile drains (at a depth of about 1 m below the surface) on the farmland, and which are surrounded by ditches, make it difficult for freshwater recharge to freshen-up the land. Much of the downward infiltrating rainwater which acts as recharge is lost in the drains or flows into ditches as it meets upwards flowing saline groundwater (saline seepage).

In Walcheren, Zeeland, local farmers in the triangle Serooskerke - Vrouwenpolder - Oostkapelle along with the Rijkswaterstaat, Deltares, Aequator, InnovatieNetwerk, ZLTO and the local waterboard of Scheldestromen, formed the Waterhouderij Walcheren (see figure 1 for the farmers involved and the location). This alliance of institutions and farmers aims to address the main issue of freshwater management and supply, as to become more independent of external freshwater sources and improve current freshwater issues. In winter, water damage to crops, due to water surpluses is not uncommon, and in summer, drought and saline seepage is often a serious problem.

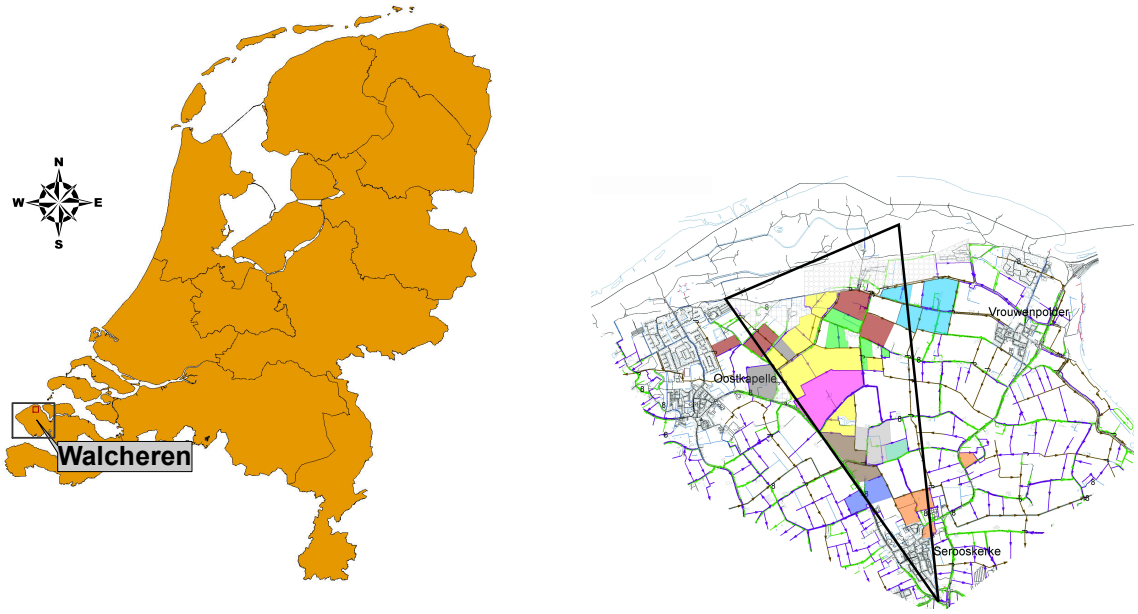

(a) Study site location in Walcheren (red box).

(b) Farmers involved in the Waterhouderij Walcheren (colored plots of land).

Figure 1: The location of the study site in Walcheren and the Waherhouderij Walcheren members, Zeeland, the Netherlands.

Farmers in the area currently incur about 10 - 30% damage to crops per year due to drought (*Van Baaren*, 2012). One of the main measures of interest in addressing the freshwater supply issue is artificial groundwater storage of surplus freshwater from seepage (out of the dunes) and precipitation (e.g., in winter) for use in times of freshwater deficits such as often occurs in mid to late summer. One of the main solutions proposed in this measure is to increase the size of freshwater lenses on fossil sandy creeks to temporarily store water for use in summer and possibly reduce saline seepage. This method is tested out in the southern plots of the Waterhouderij. In areas without fossil sandy creeks, such as in the north, the main freshwater lenses are much thinner and found on the farmlands. Increasing these smaller freshwater lenses on land is another proposed measure

for investigation, and one that is addressed in this paper. Another important measure would be to separate fresh and saline seepage water in the ditches for immediate irrigation or storage. Currently, much of the fresh water in the ditches mixes with saltwater that later contaminates the land, rendering it useless for irrigation. It is very important that the different areas of seepage of freshwater and saltwater and areas of recharge are identified so that saltwater seepage can be separated and routed away with ditches, leaving freshwater from dune seepage and precipitation for irrigation use and/or artificial recharge.

1.1 Goal

The goal of this MSc Research is to gain an understanding of the local hydrological system and research the hydrological feasibility of proposed measures to increase fresh water availability in Walcheren, specifically for the fruit plantation of Piet Korstanje and farmland of the Maljaars brothers.

1.2 Research questions

1. How does the local hydrology along the dunes and the farmland to the south of them work?
    i. What does the lateral and vertical distribution of freshwater and saltwater look like?
    ii. What is the lateral extent of the freshwater system of the dunes?
2. What are the potentially effective measures to increase fresh water availability?
    i. Are there possible changes in the surface water system that could increase fresh water availability?
    - Routing of ditch water to separate and prevent mixing of fresh and saltwater?
    - Increasing ditch water levels to prevent seepage and/or increase the thickness of the freshwater lens?
    ii. Can freshwater in times of surplus be infiltrated into the subsurface to be used in the summer dry months (aquifer storage and recovery)?

2 The study site

The study site is located in the north of the former island of Walcheren, in the province of Zeeland, the Netherlands, see figure 1. Farmers in the triangle between Serooskerke, Vrouwenpoldser and Oostkapelle along with institutions like Deltares, have formed an alliance called the Waterhouderij Walcheren. Within the framework of the Waterhouderij, a northern study site, behind the dunes and a southern study site, on a fossil sandy creek, was identified for use in two research topics for MSc students. The northern study site is the location where the research for this paper was carried out. Figure 2 shows a digital elevation map (DEM), the location of the study site, the modeled domain and the farmland of two farmers cooperating with this research.

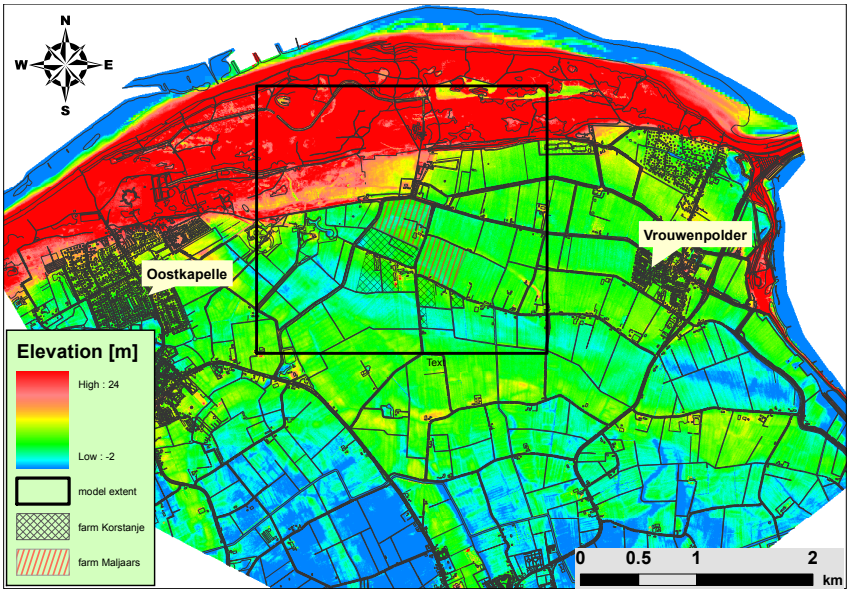

Figure 2: Digital elevation map of the study site, showing the modeled domain and the farmland of two farmers cooperating with this research. Note that this elevation map legend highlights the subtle differences in elevation around the elevation range of 2 - 0 m above NAP. The dunes reach an elevation of no more than 24 m above NAP and the elevation of the farmland is on average around 1 - 0.5 m above NAP.

The farmers, Piet Korstanje and the Maljaars brothers gave consent to carry out measurements and try potential measures as indicated by research based on field measurements and modeling results. Their plots of land are particularly interesting as they are close to the dunes and experience saline seepage. There are several reasons for this close cooperation with them, they mainly pertain to the opportunities of research on their farmland. Farmer Piet Korstanje grows apples and pears. His fruit trees are highly sensitive to fluctuating water tables and salt concentrations. In 1991, an 80 m abstraction drain at 5 m below surface level, was placed on his farmland. He extracts about 6000 m^3 of water per year for frost control and extra irrigation in summer. This amount is not nearly enough and he wishes to have access to 17000 m^3 of water per year. Mr. Korstanje has shown the potential for shallow groundwater production in the area by exploiting these freshwater lenses. Nevertheless, recently his well is increasingly producing saltier water. While avoiding local salinization of the root zone is of utmost importance, water production for his fruit orchards is a must if drought and frost damage is to be avoided. Research into artificial recharge methods could potentially increase or replenish the freshwater store and greatly benefit his farming practices. The Maljaars brothers grow an assortment of crops which have shallower rooting depths than apple and pear trees. Their land however is located in a very strong area of saline seepage and also receives a lot of freshwater from the dunes that are routed there by the ditches. This is investigated further in this paper. Also, their eastern plot of land is without drainage. This provides a good opportunity to compare freshwater lens sizes and test measures on differently drained land parcels.

3 Paleogeography, geomorphology and hydrogeology

3.1 A brief geological history of the area

To understand the current hydrology of the study site in Walcheren, one must look into the geological history and development of the Netherlands. In the Pliocene, most of the Netherlands was essentially still part of the North sea. The coastline was further east, only some of the Netherlands, close to its present day borders was above sea level. At this time, the coastline was advancing towards the north-west. In the early Pleistocene, marine influence disappeared and the Netherlands was essentially created by the progradation of a large delta complex of the 'Eastern rivers' (Elbe, Weser and Ems) and river Rhine and Meuse. Progradation continued until it peaked between 900 k and 450 k years ago, at which it is tough that the coastline had extended as far a Dogger bank (*Zagwijn*, 1989; *Post et al.*, 2003). In the Holsteinian interglacial, the sea level rose and once again inundated much of the western land. Marine deposits are found from this time, in deep valley systems left by the Elstarian glacial stage, about 300 k years BP (*Post et al.*, 2003). Such glacial-interglacial cycles continued and had a lasting effect on land, where during interglacial periods, marine conditions would prevail and marine sediments were deposited on top of fluvial, aeolian or glacial deposits. Following the Holsteinian interglacial, came the Saalian glacial (180 k - 130 k years BP), that extended up to and covered about half of the Netherlands (*Post et al.*, 2003). In the Eemian interglacial period (130 k - 110 k years BP), the sea advanced inland again covering most of western Netherlands. In the Weichselian glacial (110 k - 10 k years BP), there was deposition of fined grained aeolian sands (*Zagwijn*, 1974).

Approximately 7.5 k years before present (BP), the North sea reached its current levels. It inundated the valleys of the river systems and increased the groundwater levels. The area was poorly drained and peat formation started (Basal peat). In the Calais transgression (8 k -3.8 k years BP), sea levels continued to rise, even drowning the peat in many areas. Around 5 k years BP, many of the barrier islands had formed. Tidal inlets eroded away some of the Basal peat, but more peat formed (Holland peat). The Duinkerke transgression, which started about 3.5 k years BP, eroded much of the peat in south-western and northern coastal areas. About 1000 years BP, dunes developed atop the barrier islands and roughly 300 years later, the inland sea Ijsselmeer developed (*Post et al.*, 2003). The coastline was roughly what it is today and human activity started to have the most noticeable impact on the landscape. Humans drained the land, extracted peat, reclaimed lakes, and built dikes for polders and to safeguard from flooding. The shrinkage of clay due to compaction and dewatering, and peat extraction and oxidation caused a lot of land subsidence in the area. Creeks, gullies, tidal inlets and natural drainage channels that cut through the Holocene clay and peat deposits often filled up with sand, and can be found today to have a higher elevation than their surroundings due to this subsidence. Large fossil sandy creeks can be found to be 0.5 - 1.5 meters higher and can be seen in digital elevation maps, such as that in the bottom center of figure 2.

In the Holocene, during the Calais transgression, the province of Zeeland, in the south west of the Neterlands was submerged from about 7.5 k - 5 k years BP *Van de Plassche* (1982); *De Louw et al.* (2011). When sedimentation processes became dominant, the coast prograded and several areas rose above sea level. Peat covered Zeeland between

3800 - 2000 years BP and peat extraction in the area has been commencing since there Roman times. Between 350 and 750 A.D., Zeeland was again submerged by the sea. Then, around the year 1000 A.D., the dunes had developed and people started to reclaim land from the sea by embanking the salt marshes (supra-tidal flats) and draining them to create polders. This is nicely shown in figure 3b.

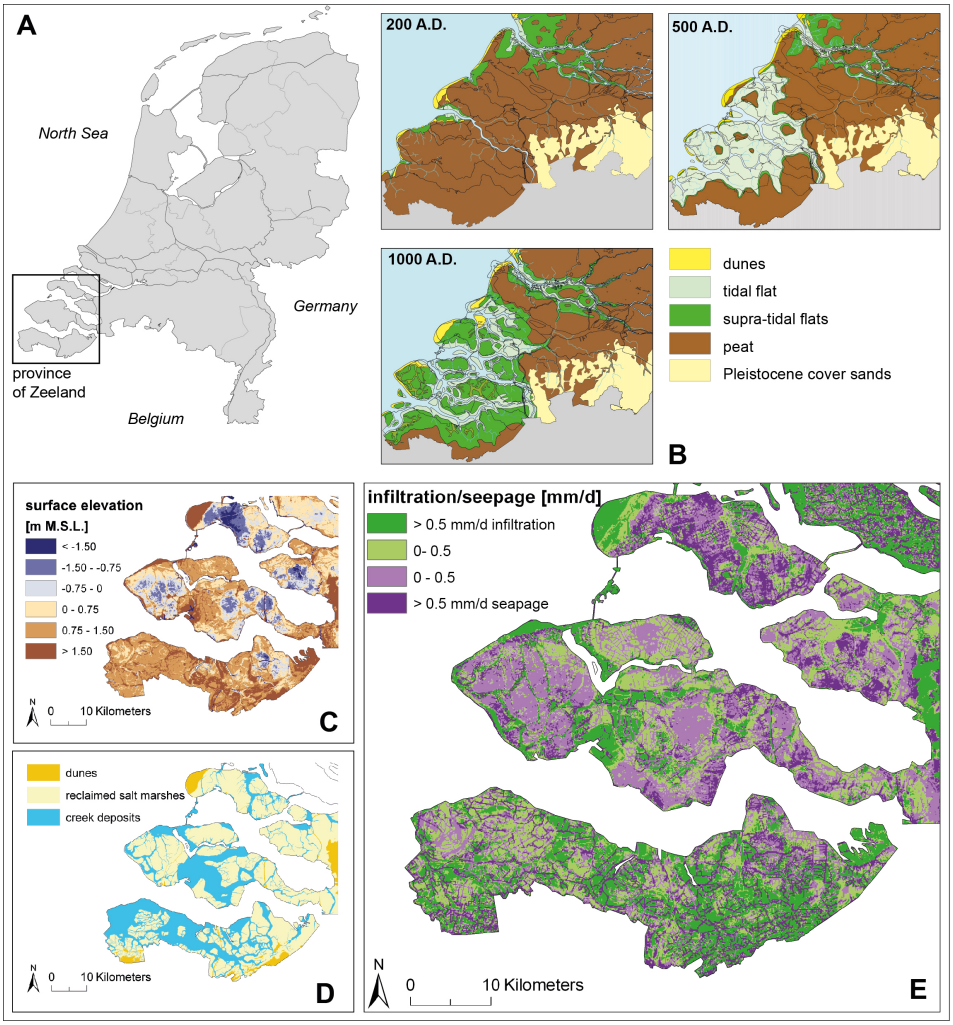

Figure 3: (a) Province of Zeeland. (b) Paleography of the study area in 200 A.D., 500 A.D., and 1000 A.D (*Vos and Zeiler*, 2008). (c) Surface elevation. (d) General location of dunes, fossil sandy creeks, and reclaimed salt marshes, based on data from REGIS II (*Vernes and van Doorn*, 2005). (e) Infiltration and seepage flux (results of regional groundwater model of *Van Baaren et al.* (2011). Taken with permission from *De Louw et al.* (2011).

Consequently we find in coastal areas of the Netherlands, that beneath the surface freshwater systems and the fresh groundwater systems (the largest ones found in fossil sandy creeks and coastal dune) there is a concentration gradient with depth, from freshwater towards that of saltwater. From the coast, this concentration decreases landwards. In general these freshwater lenses do not exceed depths of about 100 m. In the coastal areas, saltwater can often be found at much shallower depths. In the dunes of

Walcheren, north of the study site as shown in figure 1, the freshwater lens is about 40 m deep. Quite different, on farmland, freshwater lenses are typical a few meters thick (1 -10 m), and support a relative (to lens thickness) larger mixing zone. In the study area, groundwater samples from some wells less than 10 meters depth show high salinities, even within the range of seawater. In fossil sandy creeks, supported by a higher elevation and groundwater level, freshwater lenses can grow to tens of meters in size.

3.2 Hydrogeology of the area

The Netherlands is part of the subsiding North Sea basin that consists of a Mesozoic strata, overlain by Cenozoic sediments. The Cenozoic sediments vary in thickness of 400 m-1000 m (*Post et al.*, 2003). In Zeeland the impermeable base of the system is formed by low permeability Oligocene clays. These marine clays are part of the Van Rupel formaiton, and at the study site, can be found at a depth of about 80 m.

On top of the base, a layer of upper Tertiary (Pliocene and Miocene) marine sediment of sand and sandy clay makeup an aquifer. These sediments are part of the older, Van Breda and younger, Van Oosterhout formations. The top of the Van Oosterhout formation is much more clayey and can be considered a lower permeable layer. At the study site, these two formations are found from a depth of about 80 m up to a depth of around 40 - 30 m (see figure 4).

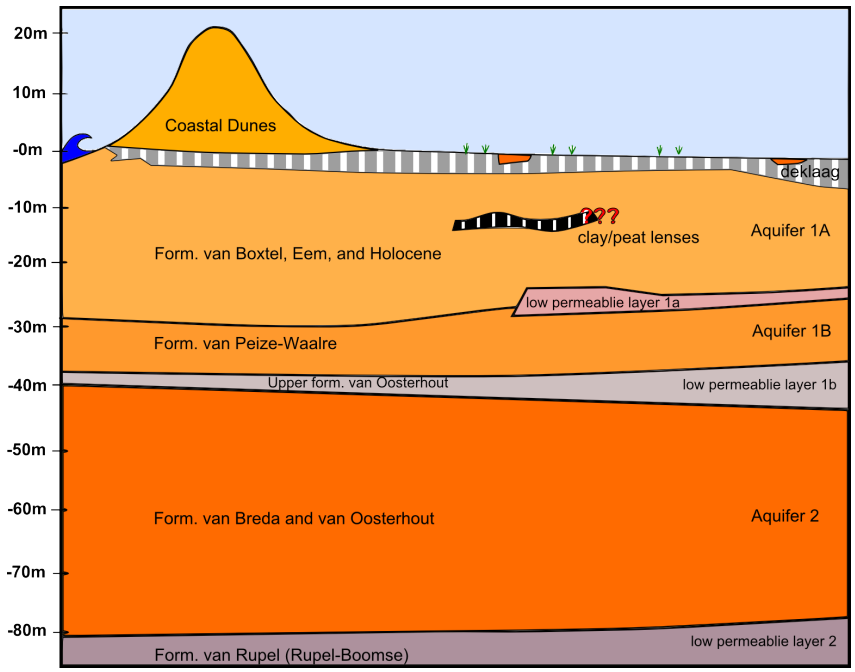

Figure 4: Hydrogeology of study site, showing the main aquifers, and confining units as well as the sedimentary formations of the study site

Above the Tertiary sediment, the base of the Quatenary deposits are represented by lower Pleistocene deposits consisting of fine-grained marine deposits that can reach up to 200 m thick in some areas (*Post et al.*, 2003). These sediments appear to be missing on a local scale at the study site.

Above the lower Pleistocene deposits, terrestrial, coarse to fine grained fluvial deposits of the rivers Rhine and Meuse are found. These deposits are known as the Van Peize-Waalre formation, and occur at a depth of about 45 - 25 m (see figure 4). They are of early-late Pleistocene age. Although a majority of this formation is of permeable sediment, and constitute an aquifer, low permeable deposits on the top of the formation sometimes occur, mainly from the more clayey Van Waalre sub-formation. This is visible at the study site, where the *low permeable layer 1a* of the Van Waalre formation is found in the sandier Van Peize-Waalre formation, *aquifer 1B* (see figure 4).

Where this low permeable layer doesn't exist, *aquifer 1B* connects to the upper aquifer, *aquifer 1A*. This aquifer is made up of upper Pleistocene and Holocene material consisting of the Boxtel and Eem formation, as well as parts of the Holocene sediments that make up the top layer. The Boxtel formation is of middle/late Pleistocene to Early Holocene age. It is generally made up of fine grained material (no larger than coarse sand) of fluvial or lacustrine origin and contains lenses of clay and peat. The Eem formation, consists of of late Pleistocene deposits of mainly coarse to fine grained marine sands with a minor occurrences of clay and shell rich layers. Aeolian and fluvial sediments from the Weichselian are commonly found on top. At the study site, the Eem and Boxtel formations are found at roughly the same depth (between 20 - 30 m), often cutting through or on top of each other. These deposits are generally found to be no thicker than 30 m (*Post et al.*, 2003).

At the surface, a Holocene layer of mixed peat, lagoonal and marine clays and fine grained sands are found. This Holocene top layer has a thickness of on average 20 m (*Post et al.*, 2003). Layering and/or lenses of sand, sandy-clay, clay and peat are often found within (see figure 4). This layer is very inhomogeneous and complex, but small pockets of sand can function as small aquifers. On a larger scale, the Holocene layer functions like a poorly connected and inhomogeneous aquifer. At the surface, the upper aquifer is semi-confined by a 1 - 5 m thick layer of Holocene age. This semi-confining layer, commonly referred to as the Holocene deklaag, consists of a highly complex configuration of peat, clay and fine grained sand. The vertical hydraulic conductivity of the deklaag is typically of magnitude 10^{-2} m/day (*De Louw et al.*, 2011). Around the north of the study site, there are coastal dunes reaching about 20 m in height. These dunes consist of well sorted sands and are covered in vegetation.

Lateral discontinuities in the lithology (especially clay and peat layers) are common on a local scale, hence hydrological parameterization of the subsurface requires a large amount of data, which is commonly unavailable. Nevertheless, on the larger scale (meters - tens of meters) some general divisions can be made between aquifer and aquitard layers and their general extent. The occurrence of clay and/or peat lenses or layers often appears sporadic but can cover significant extents. Fossil sandy creek deposits are found to cut through the upper Holocene layer in places, connecting to the first aquifer and often providing preferential flow pathways for boils to form (*De Louw et al.*, 2010).

3.2.1 Hydrology of the area

The hydrology of the area can be described as typical Dutch coastal hydrological situation. Figure 5 shows a general hydrological schematization of a coastal areas in the Neterlands. Like in figure 5, in the north of Walcheren, coastal dunes of 20 m high support a water

table which lies at about 1.5 m above MSL and a freshwater lens that reaches a maximum depth of about 40 m. These dunes were used for water production until 1995. Behind the dunes, in the low lying farmlands, the groundwater level is kept artificially low by drains and drainage ditches which channel the water to pumping stations. The pressure gradient between the sea level and the lowered groundwater level drives flow towards the land, resulting in saline seepage in the hinterlands. On the surface, rainwater meets saline seepage and contributes to a smaller freshwater lenses on top of brackish to saline groundwater. Scattered in the subsurface, clay and peat layers may form local aquitards.

Seasonal variations have a large effect on the hydrological system. On average, in winter months, recharge is positive and contributes to the freshwater lenses, while in summer, recharge is negative, due to the high evaporation and transpiration from higher temperatures and crop growth, and leads to slight contractions of the freshwater lenses. With lower values of recharge in summer, hydraulic heads in the upper aquifer and the groundwater level drop, reducing the pressure on the saltwater and often causing increased amounts of saline seepage.

Ideally, the waterboard tries to maintain higher summer ditch water levels than in winter. Promoting more drainage in winter when there is excess water and maintaining higher water levels in summer when the crops need water. However, due to the climate and farming practices, in summer water levels in the ditch tend to drop due to a water shortages and summer ditch water levels cannot be maintained. Many of the tertiary ditches even dry up in summer. Lately, with increased summer droughts, dry ditches in summer are becoming more common and saline seepage is intensifying.

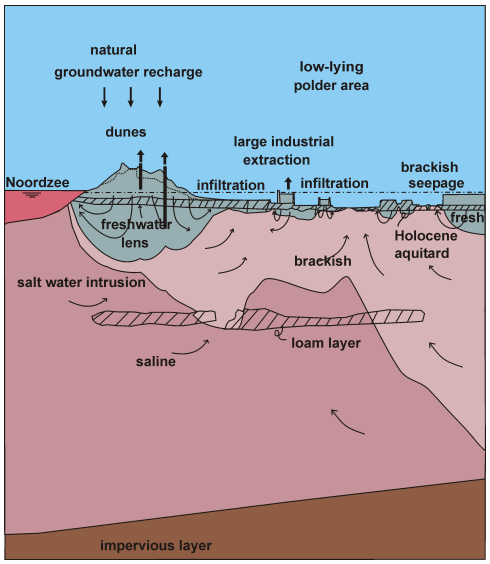

Figure 5: A Schematization of the typical hydrogeological system in coastal parts of the Netherlands, taken with permission from *Oude Essink* (2011).

Research regarding coastal aquifers and fresh and saline water interaction has become an increasingly more important field (*Post and Abarca*, 2010). Coastal aquifers are commonly characterized by spatio-temporal variations in salinity and density dependent groundwater flow. Coastal areas are typically conceptualized as an area where salt and freshwater meet, with a salt/fresh water interface dividing the two. Salinzation of coastal

lands is very common in the Netherlands. Saltwater is able to seep up in the hinterlands, behind the coastal dunes, due to the pressure gradient between the level and the phreatic groundwater level in low-lying areas. In the Netherlands, which has about 25% of its land surface below sea level, it is not uncommon for the sea level to be above the groundwater table, driving saline seepage (*De Louw et al.*, 2010; *Goes et al.*, 2009).

Research on saline seepage in the Netherlands is ongoing. Currently, processes and mechanisms of seepage and the dynamics of coastal hydrology is one of the main areas of research. Besides a small fraction of saline seepage originating by diffuse seepage, it is known that saline seepage preferentially flows along pathways of least resistance, such as through old paleochannel belts that cut through the confining Holocene layer, or through local boils (*De Louw et al.*, 2010). At the study site, several boils were observed during fieldwork and are commonly seen by the farmers during low ditch water levels or during ditch maintenance. Boils typically occur in the drainage ditches, where the water level and hence pressure is typically lower than the surrounding lands. Furthermore, considering sea level rise, it is very likely that the issue of saline seepage and the salinization of coastal areas will only become more prominent. Large dependencies on freshwater in coastal areas, such as that of agriculture, drinking water production and freshwater aquaculture will most certainly feel the pressure of sea level rise and climate change in the future.

4 Freshwater - saltwater interfaces and freshwater lens formation

The concept of a freshwater lens floating on salty or brackish groundwater can be traced back to the description of freshwater lenses on islands and dune systems by *Badon Ghyben* (1888) and *Herzberg* (1901). Consequently, this phenomena is often referred to as the Badon-Ghyben and Herzberg (BGH) principle. This hydrological phenomena is still used today and is often applied in problems involving islands (see figure 6), coastal dunes or the general case of coastal saltwater intrusion with a saltwater wedge protruding underneath the fresh groundwater (*Post and Abarca*, 2010; *Eeman et al.*, 2011).

BGH-lenses are mainly controlled by buoyancy forces of the saltwater. Like salinity stratification in the oceans, stratification can occur in the groundwater too. Assuming we start from a completely saline system, freshwater that falls on top of the system (recharge) will not fully mix with the saltwater. Instead a mixing zone will develop and stratification will occur above that. This further develops into a freshwater lens. The BGH principle states that at a reference depth, the pressure of the saline water has to equal the pressure of the fresh ground water,

$$\rho_s H g = \rho_f H g + \rho_f h g \tag{1}$$

$$h = \frac{\rho_s - \rho_f}{\rho_f} H \tag{2}$$

where ρ_f and ρ_s are the densities of freshwater and saltwater respectively, g is the gravitation constant, h is the freshwater head relative to MSL and H is the depth to the fresh-salt interface below MSL (see figure 6). In the equation above, $\frac{\rho_s - \rho_f}{\rho_f}$ is often called the buoyancy term. The above formulation, assuming a constant $\rho_f = 1000\text{kg/m}^3$ and

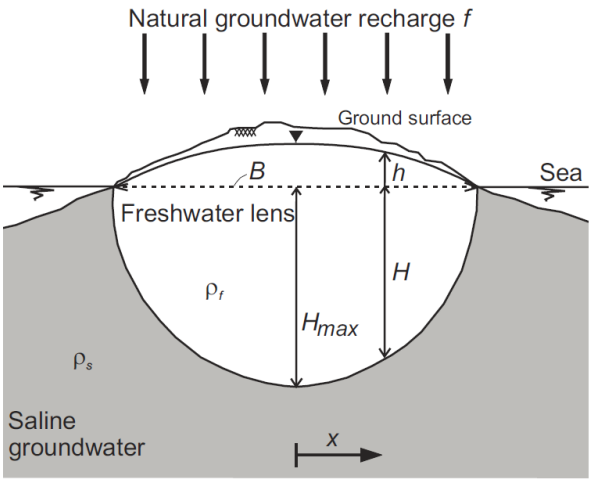

Figure 6: Fresh-salt water interface for the problem of an elongated island, showing the variables in the BGH principle. Taken from *Oude Essink* (2011).

$\rho_s = 1025\text{kg/m}^3$ can be re-written as:

$$h = \alpha H = 0.025H \tag{3}$$

Which gives the famous BGH relation $H/h = 40$, or that the depth to the interface, H, is 40 times the freshwater head, h, (or groundwater level) relative to sea level. The formulation is correct for the assumptions that the transition zone is rather sharp (in the order of several meters), there is only horizontal flow in the freshwater zone, and the saltwater is stagnant, dispersion is neglectable and the aquifer consist of homogeneous material. It is known that the solution is incorrect for the outflow zone, where in the real world we observe a protruding freshwater body from land into the sea with a certain length, however the use of the equation can give a relatively good approximation of the real situation.

Today, we observe similar phenomena on many farmland plots. In the low-lying lands behind the coastal dunes, precipitation drives freshwater lens formation on top of brackish-saline groundwater, see figure 7. The thickness of freshwater lenses can vary greatly, from a few centimeters to tens of meters (*Eeman et al.*, 2011; *De Louw et al.*, 2011). The BGH solution cannot be used accurately for shallow freshwater lenses on farmlands, as it does not capture the whole problem. It lacks an upward groundwater flow component as it assumes a vertical hydrostatic pressure distribution and hence no vertical flow. In the Dutch coastal setting, see figure 7, saltwater tends to seep up in low lying polders behind the dunes, where it meets infiltrating fresh rainwater on the land or discharges into ditches (*Eeman et al.*, 2011). The fact in the field is that the subsurface is never homogeneous, there is vertical saltwater flow, and there is not always a well defined distribution of water bodies with a sharp interface. Using numerical models, one can get a much better understanding of the dynamics of these lenses.

Eeman et al. (2011), in an numerical and analytical investigation of freshwater lens formation in typical coastal Dutch farmland, using parameter values that are typical for the Netherlands, found that the mass flux ratio, which is an indication of the upward seepage flux relative to precipitation, and the Rayleigh number, which reflects density

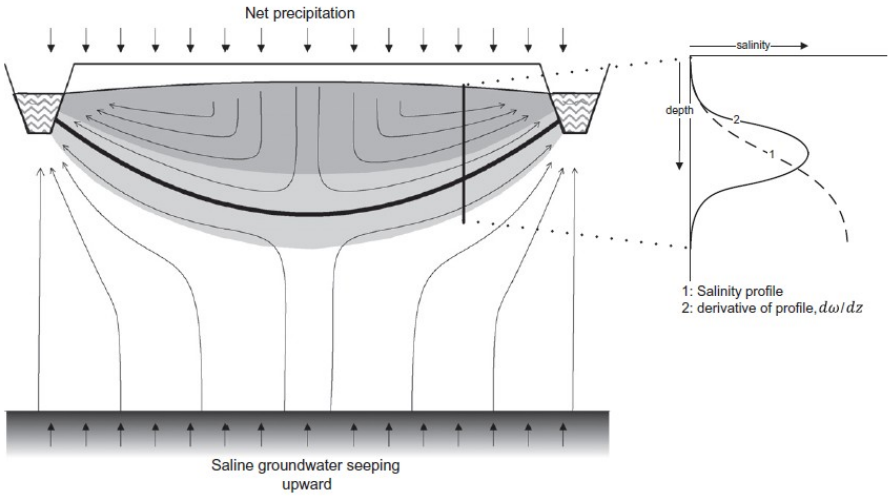

Figure 7: Conceptualized steady state freshwater lens on farmland for the typical dutch coastal setting. Freshwater lens is depicted in gray, on top of saline seepage (white), with arrows that indicate flow lines. The mixing zone (light gray) lies in between the fresh (gray) and saline water(white). Taken from *Eeman et al.* (2011).

differences, has the most significant effect on the thickness of the freshwater lens formed. They emphasized that for their reference case, when density differences were ignored, the freshwater lens became twice as thick. This finding however, would be dependent on the mass flux ratio. In areas of high seepage fluxes density differences play less of an important role. For example, according to *De Louw et al.* (2011), based on extensive field studies and numerical models, the thickness of these freshwater lenses in seepage areas depends strongly on head-driven forced convection rather than density differences between salt and freshwater. The study showed that in extremely low lying areas, where freshwater-equivalent head of brackish water in the upper aquifer is greater than that of heads in the confining top layer, freshwater lenses were on average 1.5 - 2 m thick. Whereas in higher lying areas with higher groundwater heads in the confining layer, infiltration of freshwater can form thicker freshwater lenses (5 - 15 m) as it is only constrained by buoyancy forces of the surrounding saline water.

In winter, freshwater lenses are largest; less evapotranpiration due to colder weather and no crops results in higher surface water heads and recharge rates. In summer, during times of low recharge and water levels (typically late summer), saline seepage is met with less pressure from recharge and saltwater may rise all the way to the root zones of trees and crops.

5 Artificial groundwater recharge

Artificial groundwater recharge or Aquifer Storage and Recovery (ASR), is a large area of research and has been applied successfully in many areas of the world. ASR is applied for many large scale projects to supply large water production. Typical large scale ASR projects, store freshwater by injecting it into a confined saline aquifer. The saltwater and freshwater form a mixing zone, by which they are separated. When needed this freshwater

can be pumped out. There are several other models of ASR that have been developed and are in use, see *Stuyfzand and Doomen* (2004), however the research into ASR for small scale farming purposes in low-lying, brackish, heterogeneous phreatic coastal aquifers, using freshwater lenses, such as researched for this thesis is still relatively new and revolutionary. Some examples of larger scale artificial groundwater recharge projects or sites are the Amsterdamse Waterleidingduinen along the dunes of Haarlem, the Omaruru delta in Namibia, Umudike in Souteastern Nigeria, Stockburry in the UK, Bolivar in Australia and various sites in the USA such as the San Joaquin Valley in California, the Equus Beds in Kansas and the Upper Floridian Aquifer system in Florida (*Stuyfzand and Doomen*, 2004; *Igboekwe and Ruth*, 2011; *Aiken and Kuniansky*, 2002).

The scope of this project will revolve around the concept of seasonal Leaky Storage Reservoir (LSR) combined with phreatic ASR, or LSR-ASR, a term only recently coined by *Stuyfzand* (2009) and which has become an interesting new area of research in the field of hydrology and water management. The use of small freshwater lenses on farmland plots, which are the product of a delicate balance between buoyancy forces, recharge, seepage, and drainage make this form of ASR prone to leakage, either during freshwater injection or production. The 'seasonal' term is included in the concept as the main idea here is that in the winter, when evaporation is low and precipitation leads to a lot of excess water, freshwater may be recovered from the surrounding area (e.g., ditches) and infiltrated into the ground, either by injection into the subsurface, or by maintaining higher ditch water levels to promote more infiltration and reduce drainage of the freshwater that forms the freshwater lenses in the fields. This stored freshwater could then be pumped out for farming purposes in summer, when water shortages mostly occur. By artificially injecting water into the subsurface or increasing its infiltration naturally, it is hypothesized that the size of the freshwater lenses will increase, thereby allowing for water production in times of shortages and preventing or reducing saltwater intrusion.

Although there is good documentation of large-scale artificial groundwater recharge projects and many successful results, small-scale projects in the same hydrological setting like the focus of this MSc research has not yet been carried out with great success. Some early documented attempts in the 1980s in the Netherlands that revolved around aquifer storage and recovery from fossil creek beds, concluded that the method was economically not feasible, or in some cases just unsuccessful (*Van der Straat*, 1986; *Van Meerten*, 1986). Furthermore, analytical and numerical solutions to describe the freshwater lenses were based on the the Badon Ghyben and Herzberg principle and ignored important components such as vertical groundwater flow. Although some field attempts at aquifer storage and recovery were somewhat successful, they revolved around increasing freshwater in fossil sandy creeks, different from the hydrogeological setting found at this research site, which doesn't have fossil sandy creeks cutting through the land.

The small-scale application of seasonal phreatic aquifer storage and recovery of in the Dutch saline coastal setting is of great potential importance. Should measures to increase freshwater availability in the phreatic aquifer be found effective in this research, the application could span large regions of the Netherlands and even other countries with similar hydrogeological settings.

6 Density dependent groundwater flow modeling

6.1 Theory

6.1.1 Equation of state

Density dependent groundwater flow modeling takes into account the effect of density differences on groundwater flow. Density is a function of temperature, pressure and the concentration of dissolved solids such as salts and trace elements. Generally, for the purpose of modeling groundwater flow one can neglect pressure and temperature effects on groundwater density, simplifying the density as a function of dissolved solids only.

The simplification of water as an incompressible medium is commonly made in groundwater problems, allowing for one to neglect the effect of pressure changes on density. Temperature too is often neglected as its effect on density, within the natural range of groundwater temperatures is minimal. At atmospheric pressure, within the range of groundwater temperatures (0°C - 20°C), the density of pure water varies only slightly; between 998 and 1000 kg/m^3 (*Fitts*, 2002). In fact, deeper groundwater (> 20 m) does not fluctuate in temperature (average around 10° C) as shallow groundwater and surface water which is subject to seasonal variations does (**?**).

In groundwater flow problems, the density of freshwater is taken to be a constant at 1000 kg/m^3 and the density of seawater is 1025 kg/m^3. The difference in the density between freshwater and seawater is simplified as a function of the concentration of dissolved solids only. In coastal groundwater, where freshwater and seawater mix, chloride is the predominant anion present. In seawater, chloride is present at 18630 mg/l (this is the concentration considered in this research, however this amount does vary slightly depending on location). Being the major ion in coastal waters, the distribution of chloride is most often modeled and used to infer the relative concentrations of other ions and/or the salinity. The salinity, S, is related to the chloride concentration, C, by $C = 0.544S$ (*Oude Essink*, 2011). Thus as density can be generalized to be a function of chloride concentration, we can model density dependent groundwater flow by simplifying density as a linear function of chloride concentration only. This relationship is described by the equation of state:

$$\rho(C) = \rho_f \left(1 + \alpha \frac{C}{C_s}\right) \tag{4}$$

where $\rho(C)$ is the density of the groundwater at a given concentration, C, ρ_f is the density of freshwater, 1000 kg/m^3 or a reference density, α is the relative density difference, $\alpha = (\rho_s - \rho_f)/\rho_f = (1025 - 1000)/1000 = 0.025[-]$, ρ_s being the density of seawater and C_s the chloride concentration of seawater, 18.63 kg/m^3 or a reference chlorinity.

6.1.2 Equation of motion

For density dependent groundwater flow, instead of using the classical Darcy equation for constant density, $\mathbf{q} = -\mathbf{K}\nabla h$, a more fundamental equation is needed, where groundwater density is accounted for. The more general law for flow in porous media that accounts for density dependence of flow, as presented by *Bear* (1972) is:

$$\mathbf{q} = -\frac{k}{\mu}(\nabla P - \rho \mathbf{g}) \tag{5}$$

with components:

$$q_x = -\frac{k}{\mu}\frac{\partial P}{\partial x} \qquad q_y = -\frac{k}{\mu}\frac{\partial P}{\partial y} \qquad q_z = -\frac{k}{\mu}\left(\frac{\partial P}{\partial z} + \rho_w g\right) \tag{6}$$

where q_x, q_y, q_z is the specific discharge in the principal directions, in m/day, k is the intrinsic permeability, in m^2, μ is the dynamic viscosity of groundwater, in kg/m day, P is the pressure, in kg/m day^2, ρ_w is the fluid density, in kg/m^3 and g is the gravitational acceleration, in m/day^2.

In this formulation, the driving force, the pressure, P, and the density, ρ, is needed to solve for the specific discharge, q. Principally, gathering this data is possible, however it is much more practical and common for hydrologists to formulate the equations in terms of head. Furthermore, groundwater flow code such as MODFLOW and MOCDENS3D use head data as input. To formulate the equations in terms of hydraulic head, we introduce the concept of fictional freshwater head, h_f. The fictional freshwater head equivalent can be found according to an equation, as described by *Post et al.* (2010),

$$h_f = \frac{P}{\rho_f g} + z \tag{7}$$

where, h_f is the sum of the (normalized) pressure head $P/\rho_f g$ and the elevation head, z. Also, we introduce the freshwater hydraulic conductivity, $K_f = k\rho_f g/\mu_f$, which depends on the porous medium and the freshwater properties.

By reformulating the equation above in terms of fluid pressure, P and substituting it into component equations (6) and differentiating, we get:

$$q_x = -\frac{k_x}{\mu}\left(\frac{\partial}{\partial x}(h_f - z)\rho_f g\right) = -\frac{k_x \rho_f g}{\mu_f}\frac{\mu_f}{\mu}\frac{\partial h_f}{\partial x} = -K_{f,h}\frac{\partial h_f}{\partial x} \tag{8}$$

$$q_y = -\frac{k_y}{\mu}\left(\frac{\partial}{\partial y}(h_f - z)\rho_f g\right) = -\frac{k_y \rho_f g}{\mu_f}\frac{\mu_f}{\mu}\frac{\partial h_f}{\partial y} = -K_{f,h}\frac{\partial h_f}{\partial y} \tag{9}$$

where $K_{f,h}$ is the freshwater equivalent horizontal hydraulic conductivity and it is assumed that salinity variations have a negligible effect on viscosity, such that $\mu_f/\mu = 1$. This is a good assumption for practical applications (*Post et al.*, 2010). For the vertical flow component, we get:

$$\begin{aligned} q_z = -\frac{k_z}{\mu}\left(\frac{\partial}{\partial z}(h_f - z)\rho_f g + \rho_w g\right) &= -\frac{k_z \rho_f g}{\mu_f}\frac{\mu_f}{\mu}\left(\frac{\partial h_f}{\partial z} - 1 + \frac{\rho_w}{\rho_f}\right) \\ &= -K_{f,v}\left(\frac{\partial h_f}{\partial z} + \frac{\rho_w - \rho_f}{\rho_f}\right) \end{aligned} \tag{10}$$

where $-K_{f,v}$ is the vertical freshwater hydraulic conductivity, which differs from the horizontal freshwater hydraulic conductivity, $K_{f,h} = K_x = K_y$. Furthermore, we can formulate the equations in terms of freshwater hydraulic conductivity K_f, instead of field measured values for ambient conditions of μ_w and ρ_w, because their difference is

much smaller than the uncertainty associated with this parameter, K (*Post et al.*, 2010). Equation (10) is implemented in several variable density flow and transport codes, including MOCDENS3D and SEAWAT. The extra term in equation (10), $(\rho_w - \rho_f)/\rho_f$ is the buoyancy term, as we saw in equation (2) above and is responsible for the formation of freshwater lenses. It is important to note that in calculations of horizontal flow for a given location, the freshwater head gradients (as in equations (8) and (9)) should be evaluated at the same depths.

6.1.3 Equation of solute transport

Since the only solute considered is the conservative ion chloride, Cl^-, we formulate the transport equation only for a conservative solute, neglecting reactions such as sorption, desorption and decay. This equation is also known as the non-steady state, advection-diffusion equation which incorporates the transport of solutes and the variation of densities in groundwater flow and solute transport. For three dimensions (x, y, z), using nabla (∇) notation, this gives:

$$\frac{\partial C}{\partial t} = \mathbf{D}\nabla^2 C - \frac{\mathbf{q}}{n}\nabla C \tag{11}$$

where $\mathbf{D}$ is the 3D hydrodynamic dispersion vector, $\mathbf{D} = [D_x, D_y, D_z]$, $\mathbf{q}$ is the 3D vector for specific discharge in the component directions (x, y, z) and n is the porosity.

6.2 MOCDENS-3D

For the purpose of modeling density dependent groundwater flow to help understand the hydrological situation at the study site and to test potential measures to increase freshwater availability, the numerical transport code MOCDENS3D is used. MOCDENS3D is a robust numerical transport code that is able to simulate density dependent groundwater flow. It is an adaptation of MOC3D (*Konikow et al.*, 1996) for density differences (see *Oude Essink* (1998, 2011) for more detailed information). MOCDENS3D is thus an integration of two well known and robust modules, MOC3D (adapted for density differences) and MODFLOW-96 (*McDonald and Harbaugh*, 1988). The groundwater flow equation is solved by the MODFLOW module, where density differences are accounted for through the buoyancy term, added to the RHS term of the basic flow equation (*Oude Essink*, 2011). The advection-dispersion equation is solved in two steps. The advection component is solved by MOC3D using a particle tracking technique (methods of characteristics), and the dispersion of solutes is solved by a finite difference method.

7 Methods

7.1 Field measurements

Geophysical methods were used to investigate the spatial distribution of salt in the shallow subsurface and to gain a better understanding of the local hydrology of the study site. Here, geo-electrical and electromagnetic (EM) methods were used. These geophysical methods allow for the measurement the apparent resistivity or conductivity of the

subsurface. From this, empirical relationships are used to derive the EC and equivalent chloride concentration of the groundwater or ditch water.

Geophysical methods are nondestructive and can provide a multitude of results in a relatively short time period. This was an important consideration in the planning of fieldwork. The farmers requested that non destructive methods be used, so to not disturb the subsurface in such a way as to promote an increase in saline seepage by intrusive methods that may create preferential seepage pathways. Data gathered from the field was critical in calibrating and validating the hydrological model later built.

Two fieldwork campaigns were carried out. During the fieldwork campaigns, Temparature - Electrical Conductivity (T-EC) probe, Electrical Conductivity (EC) as well as EM-31 measurements were taken to get a good understanding of the distribution of salt and areas of seepage. Then, fresh areas that could be identified were returned to for Continuous Vertical Electrical Sounding (CVES) measurements. The combination gave an excellent overview of the distribution of salt, the thickness of some freshwater lenses and provided helpful in pinpointing areas of seepage. Surface water and groundwater can then be classified into different groups based on the EC or chloride concentration (see table 1).

Table 1: Classification of water based on chloride concentrations and EC of water. Based on classifications of *Stuyfzand* (1993).

EC [mS/cm]	**Chloride** [g/l]	**Classification**
0.0 - 0.9	< 0.15	Fresh
0.9 - 1.5	0.15 - 0.30	Fresh-brackish
1.5 - 3.8	0.30 - 1.00	Brackish
3.8 - 27	1.00 - 10.0	Brackish-Saline
> 27	> 10	Saline

During the period of the research, several trips to the study site were also made to discuss the concerns as well as suggestions of the farmers in relation to this project. The farmers contributed greatly to the historical knowledge of the site, possible locations of saline seepage and information on local climate trends and typical climate conditions. Furthermore, the farmers were able to suggest several scenarios that they thought feasible to increase the freshwater lenses.

7.1.1 Electrical Conductivity

Electrical conductivity measurements of the ditch water in the central part of the modeled area was carried out in December 2011 using a high precision field EC meter. The sampling campaign followed the movement of water in the ditches. Measurements were taken 10-50 m apart as to allow a comprehensive classification of ditch waters and pinpoint areas of high salinity and possible seepage. Stratification of rainwater and brackish water in the ditches was common, consequently, EC measurements of the bottom water was recorded.

To get a more quantitative perspective of the salt distribution in the subsurface and ditches, EC measurements are converted to chloride, Cl^-, concentrations. Chloride concentrations are reflective of salinity due to the fact that chloride is the major ion in

seawater and all the major ions in seawater occur in the same relative proportions. At lower concentrations of Cl^-, competing anions such as sulphate and nitrate, play an important role in the EC - Cl^- conversion and introduce a non-linear relationship. In the Netherlands, the major competing anion is bicarbonate (HCO_3^-). This is depicted below, in figure 8. EC is typically expressed in units of Siemens per length scale (S/L). In this paper, EC is reported in units of mS/cm.

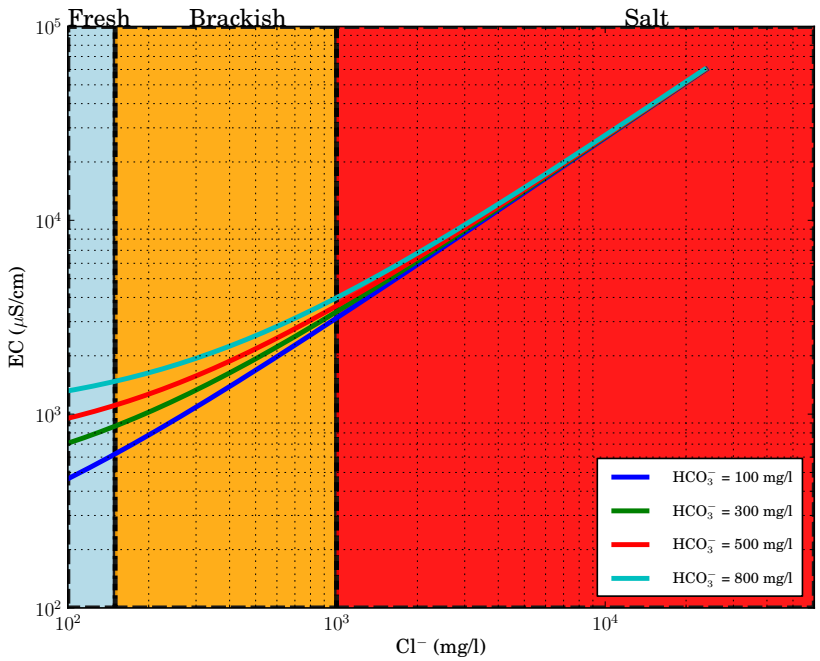

Figure 8: The relationship between EC and Cl^- as a function of different concentrations of competing ion bicarbonate (HCO_3^-), following equation (12).

EC to Cl^- conversions are calculated using a curve by the Dutch Geological Survey (TNO) as explained in their 1992 report (*TNO*, 1992) for a HCO_3^- concentration of 300 mg/l.

$$Cl^-[g/l] = \left(0.1 \times EC[mS/cm] - 0.122\frac{HCO_3^-[g/l]}{0.44096}\right)^{(1/0.9446)} \tag{12}$$

Although no water samples were measured for the exact concentration of HCO_3^-, it is known that in the coastal areas of the Neterlands, one can assume a concentration of 300 mg/l with relatively good certainty. *Stuyfzand* (1993) for example, in his extensive PhD thesis analyzed numerous polder water samples for bicarbonate and compiled literature results. Reported polder water analyses show bicarbonate concentrations in close range to the assumed 300 mg/l.

7.1.2 T-EC probe

T-EC probe measurements were carried out in the ditches within the central part of the model area to pinpoint areas of saline seepage. Hydraulic heads are lowest in the ditches

relative to the farmland plots, making the ditches the primary area of seepage. The T-EC probe measures the temperature and electrical conductivity of soils or soft sediment up to a maximum depth of four meters. In the field however, this depth is often more shallow due to the lack of physical strength required to push the probe deeper in sandy or very hard sediment. The TEC probe is made up of a titanium or stainless-steel rod and a tip consisting of two electrodes and a temperature sensor. The probe requires manual labor to push into the ground and typically measurements are conducted with 10 cm intervals. The temperature sensor is located at the tip of the rod and the two electrodes are located above the temperature sensor and are used to measure the apparent EC of the soil and pore water. The device is connected to a high precision field EC meter which can readout and standardize the EC data to a temperature of 25° C.

As the EC meter is typically not calibrated for the T-EC probe, recorded EC values have to be corrected for the device. An instrument correction factor between 0.3 and 0.5 is used depending on the salinity of the groundwater. Before the EC of the groundwater can be deduced, the resistance of the soil must be accounted for. The soil or soft sediment can typically be classified into several different groups. Based on the work of *De Louw et al.* (2011), who used the same T-EC probe device, formation factors for four different lithologies were deduced (see table 2). These formation factors were used to correct for the effect of the soil on the measured apparent EC. The EC of the groundwater is then converted to Cl^- concentration using equation (12) for a HCO_3^- concentration of 300 mg/l.

Table 2: Formation factors (FF) for different lithological units, based on the work of *De Louw et al.* (2011).

Lithology	**Average FF**
Peat	2.1
Clay	2.5
Sandy clay/clayey sand	2.8
(Clayey) fine sand	3.2

7.1.3 EM-31

The EM-31 device is an electromagnetic device which measures the bulk apparent electrical conductivity of the shallow subsurface, to a depth of about 6 m. This instrument is light weight and is designed to be carried by one person, allowing for large area and quick field surveys. The device consists of two coils on either end of a rod, connected to a field computer, GPS and a power source. An AC current is applied to the transmitting coil on one end, which creates a primary electromagnetic field that is able to penetrate the subsurface. A secondary magnetic field in the subsurface is generated which is then picked up by the receiving coil on the other end. The measured secondary magnetic field (taking into account the primary magnetic field) is then used to calculate the apparent EC of the bulk shallow subsurface. EC measurements, combined with GPS coordinates are automatically taken and logged in a field computer every second. A good idea of the spatial distribution of salt in the shallow subsurface is thus obtained. Most importantly, it allowed for the mapping of fresher and saltier areas with corresponding deeper

and shallower freshwater lenses respectively, as indicated by higher or lower conductivity areas.

7.1.4 CVES

CVES is an electrical resistivity method where multiple electrodes are connected by multi-core cables to a microprocessor, allowing for an array of measurements using a subset of the electrodes per measurement. CVES has the advantage that horizontal depth profiles are easily conducted and recorded and has a deeper penetration depth (about 25 m with the setup used). Electrodes can function as either current or potential electrodes. One can use several electrode configurations, however the Wenner (faster) and Schlumberger (better resolution) are commonly used. The microprocessor and software use numerous combinations of current and potential electrodes to calculate the apparent resistivity of the subsurface. Inversion software is then used to build a two-dimensional, layered, model of the subsurface apparent resistivity along a transect of the setup electrodes. For the CVES measurements reported here, the Schlumberger configuration was used.

Typically, to remove the effect of the sediment on the measured apparent resistivity, formation factors for the subsurface n-layered model are needed in the conversion to resistivity. This data would have been expensive and required a lot of field work to compile. As the shallow subsurface at the transect locations have formation factors that range between that for clay ($FF = 2.5$) and that for (clayey) fine sand ($FF = 3.2$), results would not change significantly. Being mainly interested in the depth to the freshwater lens, the contrast in resistivity between fresh and brackish groundwater is great enough to override any significant errors the sediment might have on the modeled interface depth.

7.2 Model Setup

To gain a better understanding of the hydrological system of the interest area around the farms of Piet Korstanje and the Maljaars brothers and to test possible measures to increase freshwater availability, a 3-D density dependent groundwater flow model was setup using the numerical transport code MOCDENS3D. Table 3 and table 4 summarize the spatial discretization used and the physical model buildup, while table 5 lists the parameters used in the building the numerical model. These are all further discussed below.

7.2.1 Domain and time discretization

A model of 5.75 km^2, extending from the dunes, north of the farms of Piet Korstanje and the Maljaars brothers, into the low lying, reclaimed marshes (now farmlands) with dimensions of 2500 m (E-W) by 2300 m (N-S) was decided upon. The large size was to ensure the model boundaries are far enough from the area of interest and that mistakes made at the boundaries (e.g., boundary conditions) do not effect the model results in the interest area to a significant degree. The ideal distance between the model boundaries and the area of interest in the center of the model (3λ) was calculated according to the formula $\lambda = (T \times R_v)^{1/2}$, where T is the upper aquifer transmissivity, and R_v is the vertical resistance of the deklaag. Remaining conservative, a transmissivity of 400 m^2/day ($\mathrm{T} = 10\,\mathrm{m/d} \times 40\,\mathrm{m}$) and resistance of 200 days ($R_v = \mathrm{h_{deklaag}/k_v} = 5\,\mathrm{m}/0.05\,\mathrm{m\,day^{-1}}$)

was used to calculate a 3λ of 600 m. The models northern boundary was made to extend into the dunes so that the hydrology of the dunes in the area and their effects on the farmlands could be better understood. Initially, using the water divide of the dunes was thought to be a good model boundary. Later during the data collection period, having found no exact information on the location of the divide, this idea was eliminated.

Table 3: Model dimensions and horizontal domain discretization

Description	Value
N-S extent	2300 m, 230 cells
E-W extent	2500 m, 250 cells
Cell size (horizontal)	10 m $\times$ 10 m
Vertical extent	89.5 m
layers	66
Top elevation	2.5 m rel to NAP
Bottom elevation	-87 m rel to NAP

According to the hydrogeology of the area, the model was made to extend to a depth of 87 m below NAP where the impermeable Van Rupel formation makes for a good bottom confining unit. This depth ensured that the freshwater lens of the dunes and farmland could develop fully and that saline seepage from below could be properly modeled. The top of the model has an elevation of 2.5 m above NAP, well below the dunes, but still above the water table of the dunes. The model does not consider the unsaturated zone, and only groundwater recharge (precipitation minus evapotranspiration) is modeled.

The model area was divided into 10 by 10 m cells and vertically the model is divided into 66 layers, with the top 45 layers having a thickness of 0.5 m (2.5 m to -20 m relative to NAP) and then gradually becoming thicker (see table 4) until the bottom layer, which has a thickness of 10 m. The model grid consists of a total of 3,795,000 cells.

Table 4: Vertical discretization of model domain into 66 layers, extending from 2.5 m to -87 m relative to NAP

Layer no.	**Thickness [m]**	**Extent [m] rel. to NAP**
1 - 45	0.5	+2.5 to -20
46 - 54	1	-20 to -29
55-60	2	-29 to -41
61, 62	4	-41 to -49
63	8	-49 to - 57
64-66	10	-57 to -87

For long model runs, or salt runs, the model was run using six month stress periods and one month time steps. Half year stress periods were chosen to accommodate the two seasons of summer and winter, where the most important differences in drainage levels (in Dutch *winterpeil* and *zomerpeil*) and recharge (mainly from evapotranspiration changes) can be reflected in the model.

Density dependent groundwater flow modeling relies on the head gradients to drive flow, after which transport steps calculate particle transport (chloride movement) which

in turn, through density changes also effects the head gradients. Monthly time steps were chosen to give a high resolution, allowing for transport steps to readjust to changes in concentrations and head. For salt runs, monthly time steps with half year stress periods proved ideal in computation time and model results. For scenario runs, where the system was subject to small changes, the model was run using weekly time steps and stress periods. This was required to properly model and understand/observe the effects that small changes (in accordance to scenarios being tested) have on the evolution of the freshwater lenses and the surface freshwater system in general.

7.2.2 Hydrogeological schematization, parameterization and MOCDENS3D input parameters

Hydraulic conductivity The hydrogeological schematization and parameterization was based on the above discussed local hydrogeology of the area (see section 3.2) and the dutch Geohydrological Information System REGIS II (*Vernes and van Doorn*, 2005) as well as the mean result of 50 realizations for hydraulic conductivity (based on the Dutch geohydrological models GeoTop and REGIS) as supplied by the Dutch Geological Survey (TNO). The supplied mean hydraulic conductivity model was developed by TNO for the province of Zeeland for the use in hydrological models such as developed by *Van Baaren et al.* (2011). This 3-D hydraulic conductivity model was made up of 100 by 100 m cells, with variable cell thickness. For the purpose of this research, the hydraulic conductivity map was adjusted for cell sizes of 10 by 10 m and the layer thicknesses by layer-wise interpolation. By interpolation, sharp boundaries in the smaller resolution model could be made gradual and numerical errors and computation times from the transport model reduced. Initial model results using the mean hydraulic conductivity model produced many strange model results (discussed later) that were incorrect. As such, the hydraulic conductivity map was manually adjusted or calibrated according to the documented local hydrogeology (as discussed in section 3.2), soil maps and model results. The vertical hydraulic conductivity of the deklaag material ranges between 0.01 and 0.05 m/day and the vertical hydraulic conductivity of the dune sands ranges between 2 and 3.69 m/day.

First active (top) cells and IBOUND The first active cells (or top-cells) in the model discretized domain and the IBOUND array for MODFLOW, was based on a Digital Elevation Map (DEM) of 5 by 5 m resolution for Zeeland. This map was clipped and extrapolated to 10 by 10 m cells for the model area and capped at a maximum elevation of 2.5 m above NAP. The IBOUND array in MODFLOW indicates the active model cells. The only inactive cells in the model domain are those with elevation above the DEM. The first active cells array correlate to the top active cells of the IBOUND array. They form the model terrain and are used for placement of recharge, drains and ditches.

Starting heads and concentrations Starting concentrations equivalent to that of seawater (chloride concentration = 18.63 g/l) in the entire model domain and starting heads from the regional hydrological model of Zeeland (*Van Baaren et al.*, 2011) were used in initial model salt runs, where the model was run for 100 years to attain an equilibrium groundwater chloride distribution and hydraulic heads. Scenario model runs were started using the results of the long salt runs.

Model boundary conditions Along the models vertical boundaries, the General Head Boundary (GHB) package was used to simulate head-dependent flux boundaries. Initially, the equilibrium hydraulic heads from the regional hydrological model of Zealand were used for the GHB package heads. However, model results (of 100 year salt runs) showed problems in accurately modeling the freshwater system of the dunes; the dune freshwater lens was modeled as being too shallow. Using a hydrostatic head distribution in the GHB package for the North boundary, where the dunes were present, gave much better model results and an accurate depiction of the freshwater system of the dunes. The approximate size of the dune FWL was based on several groundwater wells and water analyses from the Dutch Geological Survey (TNO) website: DINO*Loket* (available at dinoloket.nl). Information on groundwater heads in the dunes was sparse and not enough to construct the hydrostatic head distribution along the model boundaries. Therefore, for an initial try, similar to the BGH relation, knowing the size of the dune FWL, the ratio between the maximum hydraulic head in the dunes, ≈1.5 m, and the depth of the FWL, ≈40 m, (1.5 m/40 m = 0.0375) was calculated and used to determine the surface freshwater heads along the horizontal dune-model boundaries. Based on the calculated heads in the FWL, the vertical hydrostatic head distribution of the saltwater (below the FWL) could be calculated per layer for every dune-model boundary cell using the vertical flow equation that accounts for density differences:

$$q_z = -k\left(\frac{\partial h_f}{\partial z} + \frac{\rho - \rho_f}{\rho_f}\right) \tag{13}$$

where q_z is the vertical component of the specific discharge or Darcy velocity, h_f is the freshwater head, z is the elevation head and $(\rho - \rho_f)\rho_f$ is the relative density contrast that accounts for the buoyancy effect on vertical flow. Assuming hydrostatic conditions, $q_z = 0$, the change in freshwater head, dh becomes, $dh = -dz * ((1025 - 1000)/1000)$. This was used to calculate the change in heads for the northern model boundary in every layer from the calculated head in the top cell (knowing the dz between all layers)

After several GHB head calibrations to adjust for discrepancies between observed and modeled results, equilibrium head and concentration results from the long salt runs were then used for scenario model runs.

Recharge Recharge data was based on precipitation and evapotranspiration data from the Dutch meteorological station in Vrouwenpolder and Vlissingen, respectively. Data from the period 1980 - 2010 was averaged for summer and winter days and adjusted for crop factors, dune vegetation and average water deficits. Average daily recharge for summer and winter periods used in long salt runs are -0.2 mm/day and 1.4 mm/day respectively, giving an average yearly recharge of 0.6 mm/day. However, initially, due to negative summer precipitation, the freshwater lens in the dunes developed too shallow. It was assumed that due to the dune vegetation, the height of the unsaturated zone and the high permeability of the dune sands, evapotranspiration in the dunes was likely lower than on the farmland. In the modeled dunes, summer recharge was capped at a minimum of 0.02 mm/day.

Ditches The local waterboard of Scheldestromen supplied geographical information maps of the location, types and water levels of ditches (primary, secondary and tertiary)

of the modeled area. These maps were converted to raster maps of 10 by 10 m cells for the model domain, one containing the length of ditches per cell, another, the type and two different maps for the winter and summer ditch water levels (*winterpeil* and *zomerpeil*). These maps were then used to place ditches (layer, row, column, water level and river bottom elevation) and calculate their conductance within the cells of the hydrological model. Ditches were added to the model using the river package, where information on the type of the ditch was used to determine its water depth and width. In the model, primary ditches have a width of 1.75 m and depth of 0.8 m. Secondary ditches have a depth of 1.2 m and width of 0.6 m. Tertiary ditches have a width of 0.6 m and depth of 0.3 m. Ditches are relatively small in the model area as the location is the beginning of the drainage network. The depth of the ditch below the surface determined the layers to place the ditch in for every surface cell that a ditch is present in. The conductance of the ditches in every cell is calculated based on the wetted perimeter per cell divided by a resistance value that is calibrated by several model runs (a range for resistance values have been established by Deltares from several groundwater models in Zeeland). The river stage is based on the maintained winter and summer ditch water levels (*winterpeil* and *zomerpeil*).

Drains Tile drainage is typically used on farmlands in Zeeland where drainage is required to maintain lower water levels or to increase drainage times as to avoid water damage to crops. Drainage is used on plots of land which are typically lower lying and more clayey in composition (more difficult to drain naturally). Drains are typically placed 10 m apart and no more than a meter below the surface. With the help of the farmers, plots of land which were drained or not, were identified and implemented in the model. Drains are placed 0.9 m below the surface and given a length of 10 m per cell in the drain package. The conductance of drains was calculated based on the circumference of drains (c), length per grid cell (L) and a resistance value (r, which was calibrated by several model runs), where conductance, $C = (c \times L)/r$.

Molecular diffusion and dispersion coefficient Longitudinal and transversal dispersivities used in the model is 0.1 m and 0.01 m respectfully, giving a transversal to longitudinal ratio of 0.1. For large model domains and long simulation periods, such small dispersivity values are not uncommon. A number of case studies conducted in Belgian and Dutch aquifer systems with marine and fluvial deposits report similar dispersivities (e.g. (*Stuyfzand*, 1993; *Lebbe*, 1999; *Van Meir*, 2001; *Oude Essink*, 2001; *Vandenbohede and Lebbe*, 2007; *De Louw et al.*, 2011). The molecular diffusion coefficient, D_m, was assumed to be $8.64 \times 10^{-5}\,\mathrm{m}^2/\mathrm{day}$.

Transient parameters For transient simulations, a specific yield of 0.15 was used for the top-most active cells and a confined storage coefficient of 1×10^{-5} was used for the rest of the model cells.

Table 5: Parameters and their values used in the 3-D density dependent groundwater flow model for use in numerical transport code MOCDENS3D.

Parameter	**Description**	**Units**	**value**
R_s	recharge (summer averages)	mm day^{-1}	-0.2
R_w	recharge (winter averages)	mm day^{-1}	1.4
R_{conc}	Cl-conc of recharge	mg/l	20
k_h/k_v	anisotropy factor for $k_v < 8$	-	3
k_h/k_v	anisotropy factor for $k_v \geq 8$	-	1
S_y	specific yield, upper active cells only	-	0.15
S_s	confined storage coefficient, all other cells	-	1×10^{-5}
ϕ	porosity	-	0.35
GHB_{cond}	GHB conductance (not in dunes)	m^2/day	0.1
$GHB_{cond-dune}$	GHB conductance (in dunes)	m^2/day	10
$Cl_{GHB-dune}$	Cl-conc of GHB (dune FWL)	mg/l	20
Cl_{GHB}	Cl-conc of GHB (not dune FWL)	mg/l	18630
Ω_{ditch}	drainage resistance ditch	days	3
Ω_{drain}	drainage resistance drain	days	1
h_{drain}	depth of drains	m	0.9
D_m	Molecular diffusion coefficient	m^2/day	8.64×10^{-5}
α_L	Longitudinal dispersivity	m	0.1
α_T	Transversal dispersivity	m	0.01
α_L/α_T	Dispersivity ratio	-	10
h_c	head closure criterion	m	1×10^{-6}

8 Results and Discussion

8.1 Field measurements

8.1.1 Electrical conductivity

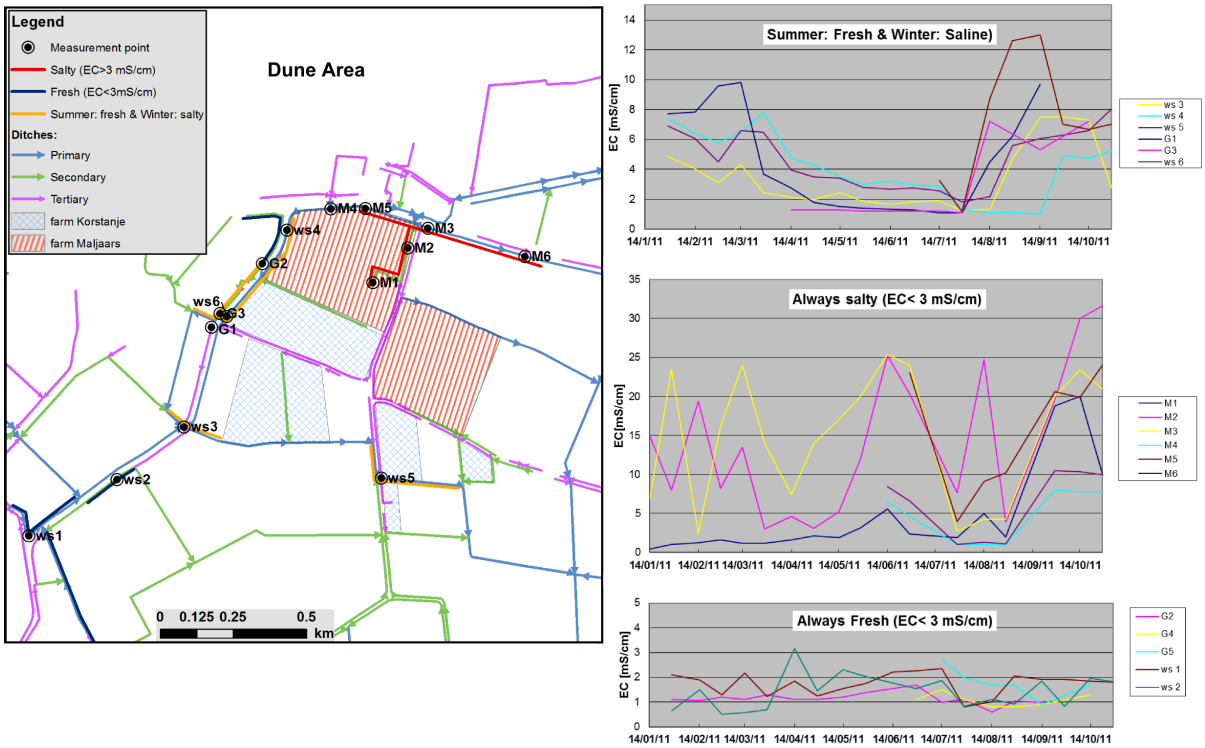

Figure 9: Ditch characterization into fresh, salty and summer: fresh and winter: salty, according to bi-monthly EC data obtained from the farmers of the Waterhouderij Walcheren. The direction of flow in the ditches is indicated. Notice that, here, freshwater is classified as having an EC of < 3 mS, this classification of freshwater is based on the recommended average crop threshold for irrigation water.

Deltares, along with the help of the farmers of the Waterhouderij Walcheren, measured the EC of ditches every couple of weeks for the period of 14 January 2011 - 21 October 2011. A plot of the EC of ditch water, as measured in several different locations over this period can be found in figure 9. The ditches can be classified into three; (1) ditches that are fresh over summer and (most of) winter, (2) ditches that are always salty or saline, and lastly, (3) ditches that are fresh in summer and saline in winter. Ditches that are fresh are located (upstream) away from areas of saline seepage. The water in these ditches could be used for the purpose of ASR. The ditches that are fresh in summer and saline in winter occur when the drainage ditches become cutoff from one another due to low water levels, and saline water that seeps upstream doesn't contaminate water downstream. The ditches are poorly connected north of measuring point $ws3$ as deepening of the ditches has resulted in ditch bottoms having lower elevations than the divers that connect them through access routs to fields that cut off the ditches. When water levels drop below the level of the divers, flow is cutoff. The ditches that are always salty are most likely the

key areas where saline seepage occurs. This helped pinpoint fresh and seepage areas for further fieldwork investigations.

EC measurement locations in the ditches and the corresponding chloride concentrations for an extensive measurement campaign conducted during fieldwork (in winter) are shown in figure 10. These measurements, point to four areas (brackish-saline to saline measurement clusters) where seepage is most likely concentrated. Looking at figure 9 above, one can see that the saline areas are all connected by the ditches and flow direction. Starting from the secondary drainage ditch where measurement point $M1$ is located, we see that water flows to $M2$ and then into the primary ditch, where it flows towards, $M5$, $M4$, $ws4$, $G3$ and $ws3$ where it then enters a very large primary ditch and flows to $ws5$ and turns south to leave the area. Upstream of (and all ditches north of) $ws3$, ditches are relatively small, as the drainage network begins in this area. Water drians to the south, before it is routed to the East and is pumped into the Oosterschelde in Veere (not shown in the maps). Only after flowing into the primary ditch after $ws3$ are the ditches large and deep enough and well connected such that flow is not disturbed when water levels drop in summer. For this reason, during summer, salty waters appear to be contained to ditches north of $G1$ and in winter the saline seepage can flow south.

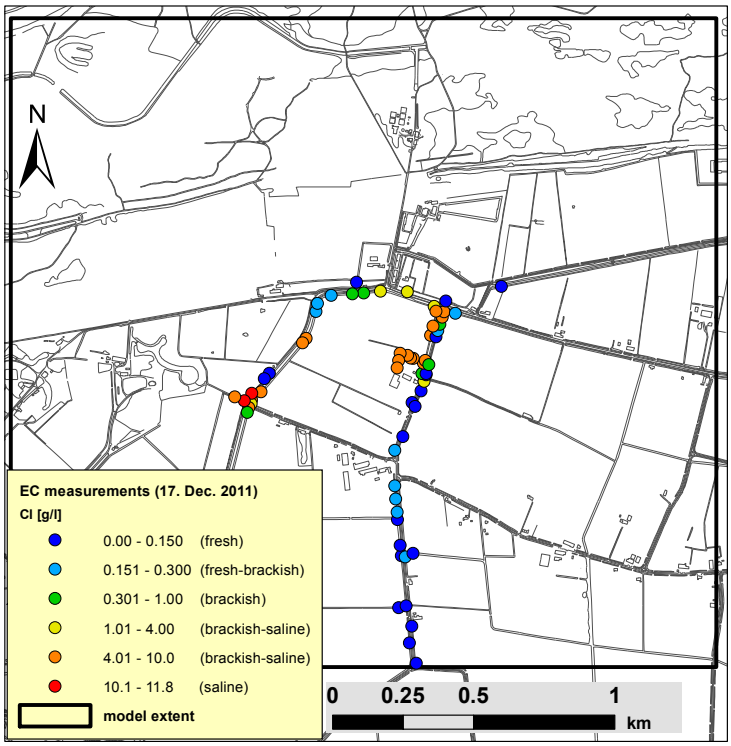

Figure 10: Cl^- concentration in ditches, based on EC measurements taken on the 17 December 2011 with ditch water chloride concentration classifications based on *Stuyfzand* (1993).

8.1.2 T-EC probe

Using the T-EC probe, saline areas as indicated by the EC measurements were further investigated to confirm suspicions of saline seepage. Figure 11 shows chloride concentration

profiles in the shallow groundwater from T-EC probe measurements in several ditches in the study area. A total of 26 T-EC probe measurement points were planned for, however only eight profiles were successful due to difficulties in penetrating the shallow subsurface in sandy areas. The classification of the T-EC probe profiles into fresh, fresh-brackish, brackish and brackish-saline profiles is according to the concentration of water at depth, where it can be assumed that the effect of the surface (ditch) water is not present. During the measurements, several upward flowing groundwater boils were observed. Not all of them presented to be saline seepage. The measurements at the surface (depth = 0 m) is the Cl^- concentration of the ditch water.

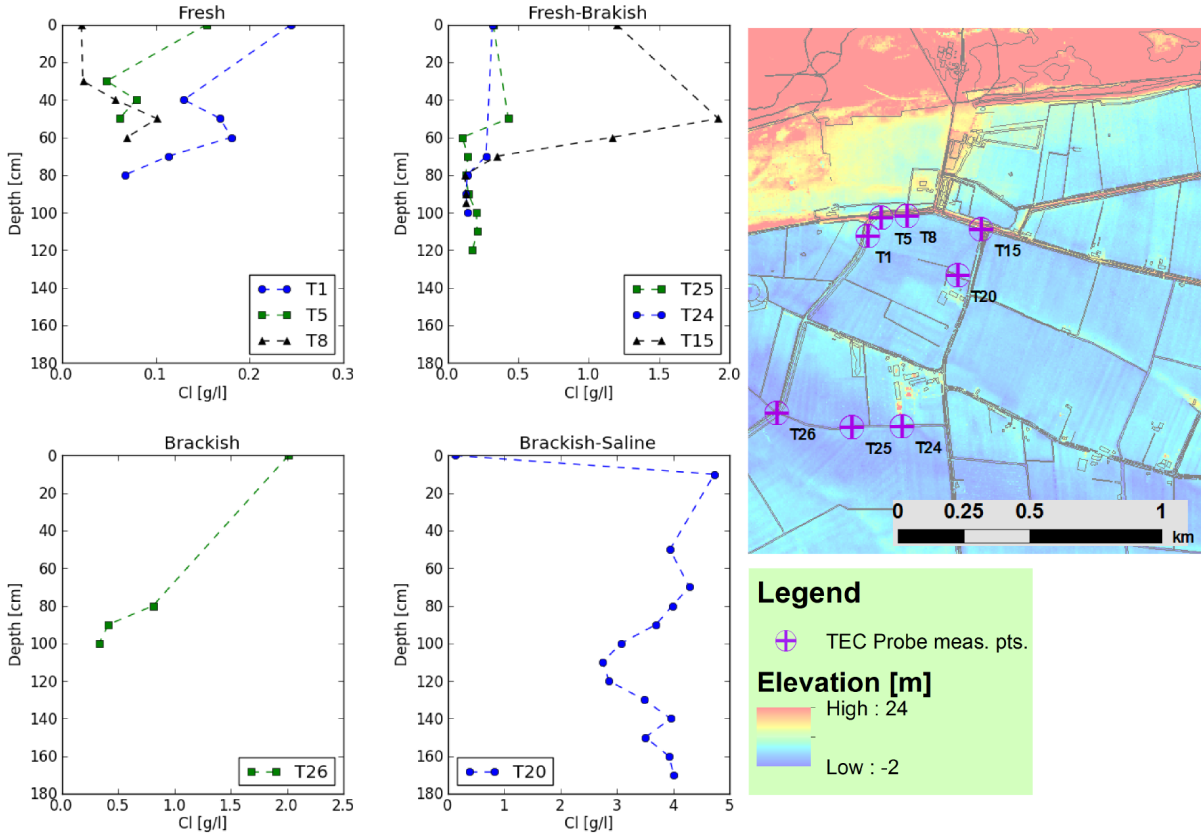

Figure 11: T-EC probe profiles of shallow groundwater taken in several ditches in the study site. Profiles have been subdivided into 4 different classes, fresh, fresh-brackish, brackish and brackish-saline, according to Cl^- concentration classifications of groundwater (see table 1). The location of the T-EC probe measurements are shown on top of an elevation map. Depth [cm] is measured form the surface of the ditch water.

We see that for the first three classifications of the the Cl^- concentration profiles, fresh, fresh-brackish and brackish, the concentrations of the surface water is higher than what it is at depth (except for T1). This is because the ditch water has been contaminated elsewhere and the Cl^- transported by the ditch water. In fact in areas with more stagnant water, stratification in the ditch water was commonly observed (e.g., T1 and T20), where rainwater had stratified on-top of the older an more saline ditch water. Profiles T1, T5 and T8 show fresh groundwater, all converging to a value of less than 0.1 grams Cl^-/liter at depth. This is in good agreement with the EC measurements. Profiles T15, T24 and

T25 show fresh-brackish water at depth. Profile T15 shows overlying groundwater that is more saline that must have infiltrated when ditch Cl^- concentrations were higher, for example over summer. The fresh, fresh-brackish and brackish profiles do not suggest saline seepage as they are either fresh or their concentrations decrease with depth. A typical saline seepage profile looks like profile T20. Where at depth and all the way to the ditch bottom the Cl^- concentration is relatively equal. At the surface, freshwater was measured stratified on top of the saline seepage. A straight concentration profile implies saline seepage due to the obvious fact that upward flowing groundwater creates a linear concentration profile of a concentration equal to the upward flowing saline groundwater. As the use of the formation factors to correct for the effect of the sediment on the the measured EC was not based on any concrete model of the subsurface, slight variations are possible. However, the small uncertainties in the formation factors would have only a minor effect on the point EC to Cl^- concentration conversion, and most certainly not change the conclusions made from these results.

8.1.3 EM-31

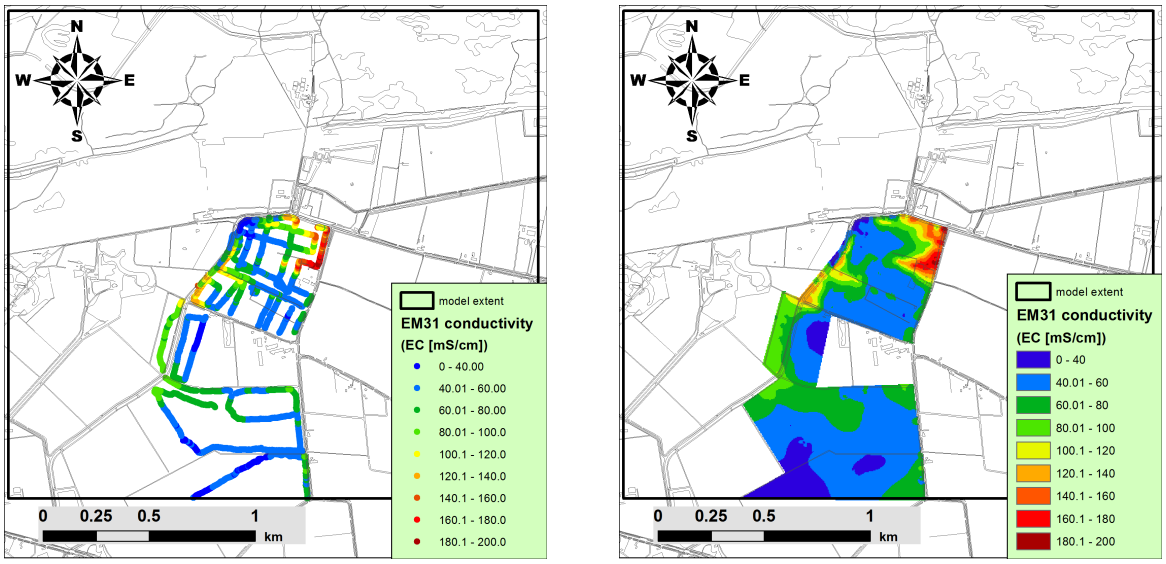

(a) EM-31 point measurements.

(b) EM-31 interpolated results.

Figure 12: EM-31 measurements showing point data and interpolated data.

EM-31 point measurements and interpolated results are shown in figure 12. Point data was interpolated using spline interpolation in ArcGIS for a defined area. As formation factors for the shallow subsurface was not available, the results still project the effect of the formations on the apparent EC. Never the less for the purpose of mapping fresh and salty areas (relative to one another), it can be safely assumed that the effect of the groundwater salinity on the measured EC is dominant over the effect of the different sediments. The data presented gives a good reflection of what is typically expected from such an area (see figure 7 for a schematization of the field situation). It is evident that close to the ditches, where the freshwater lens is thinnest, and the effect of saline ditches are present, measurements show higher EC, pointing to more saline areas and thus thinner

freshwater lenses. In the middle of the fields the freshwater lenses are thickest and EC measurements show low conductivities. The lower conductivities (blue) point towards a freshwater lens that is expected to be greater than six meters (below ground level) in depth.

A high correlation between proximity to ditches and saline groundwater occurring at shallow depth (or very shallow freshwater lenses) is observable. In several areas, notably the North-East and South-East of Maljaars North plot of land (Northern most plot of land in the EM-31 survey, figure 12, or as shown in figure 2) and the Eastern part of Korstanje's land (indicated in figure 2), the measured apparent conductivities are extremely high. Besides indicating that these areas are more saline relative to the other mapped areas, they are (most) potentially the areas of saline seepage. Saline seepage, although preferentially occurs in the ditches can also occurs as diffusive seepage under the farmland plots. This is also very clearly evident in the EM-31 results.

8.1.4 Seepage areas

Comparing the EM-31 data to the T-EC probe and EC data we see good agreement between possible areas of seepage. Not all the desired measurement points for the T-EC probe could be investigated due to the difficulties with penetrating sandyer areas, however, overall, by combining the results, the areas of saline seepage become quite clear. Three areas can be classified as areas of saline seepage, with good certainty (see figure 13).

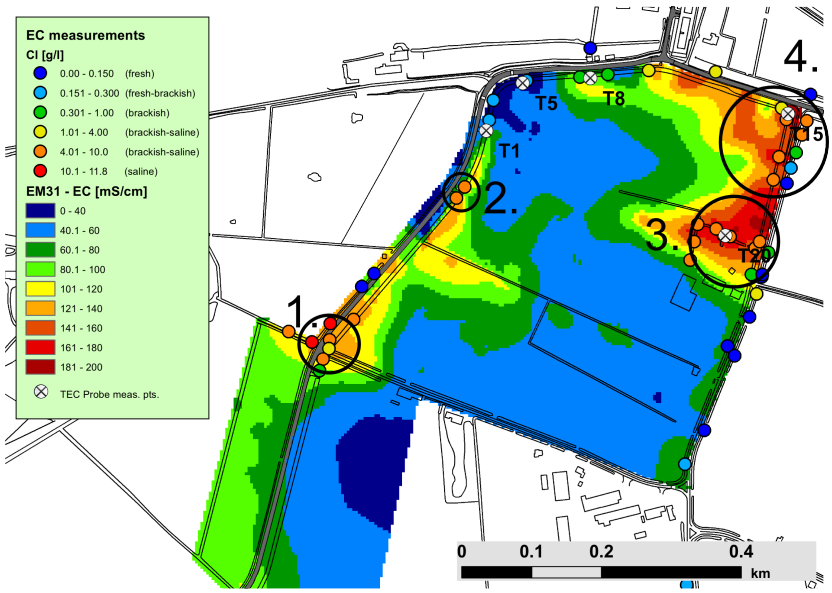

Figure 13: EC and EM-31 results and the location of T-EC probe measurements showing three areas of high certainty of saline seepage (areas 1,2 and 3) and one area of low certainty of saline seepage (area 4).

Area 1, an intersection for seven ditches, registered the highest measured EC (derived) Cl^- concentrations and relatively high EM-31 conductivities. T-EC probe measurements failed to penetrate deeper than a few centimeters, giving only partial data, however by the experience of the farmers, and the fact that this ditch was deepened several days

prior to the first fieldwork (17 December 2011, after the bi-monthly EC measurements) this area is very likely an area of saline seepage.

Area 2, in the ditch to the east of the road, shows good likelihood of being a location of seepage based on the EM-31 and Cl^- concentration data. The T-EC probe was not able to penetrate the ditch bottom here, but the presence of boils and strong stratification as well as fresh upstream water, suggest this location as another area of seepage. Though, based on the small contaminated area and minimal spreading, it is thought that the seepage fluxes are not very high. Never the less, it could also be that the presence of high saline water along the ditch bottom is a remnant artifact of the very dry summer, whereby saline water collected and remained in depressions of the ditch bottom. Further investigation in this area by the farmers could be beneficial to clarify the exact situation.

Area 3, where T-EC probe profile T20 was taken, is a certain location for saline seepage. Besides the T-EC probe Cl^-profiles showing the typical profile of a saline seepage area, EM-31 and EC measurements all point towards this ditch being a most certain location for saline seepage. It is also one of the drainage system sources/beginnings and in the field one can observe a large pond where profile T20 was taken. This area was heavily stratified, with fresh (rain) water on top of almost saline water. From the fieldwork investigations, it appears that this secondary ditch contributes saline water to a large part of the drainage system on Maljaars northern most plot of land. Being the start of the drainage system, and protruding into the fields, water comes from the surrounding farmland and saline seepage. This water then flows to the roadside ditch and turns north to the drainage junction where we also observed high Cl^-concentrations but a non seepage like (T-EC probe) Cl^-profile. This water meets incoming fresh water from the polder north of the main road (colored gray) and flows east or west in the primary ditch.

Area 4, where T-EC probe profile T15 was taken appears as a large potential area for saline seepage. However EM-31 and EC measurements show slightly lower conductivities and chloride concentrations compared to area 3, suggesting that the chloride found here could originate from the strong saline seepage area 3 upstream. This is further supported by Cl^-profile T15 (see figure 11) which is not indicative of saline seepage. In fact, profile T15 shows brackish ditch water and almost fresh groundwater at depths below 0.8 m. It is very probable that chloride seeping form area 3, flowing downstream, has, over the years contaminated the land bordering the ditches. Of course it is still possible that this area could be an area of saline seepage in the ditches or more diffusive saline seepage on land next to the ditches. To be certain, it would be recommended to place a temporary dam between area 3 and area 4, allowing for the determination of a seepage source in area 4 (see section 8.2 for more information)

8.1.5 CVES

CVES measurements gave a good impression of the depth of the freshwater lenses on Korstanje's and the Maljaars' land. Figure 14 shows four CVES profiles, one conducted on the Maljaars' land (profile A) and three conducted on Korstanje's land (profiles B, C and D). The profiles show the apparent resistivity of the subsurface up to a maximum depth of 27m. From the surface, downwards, the resistivity decreases as the groundwater transitions from fresh to saline. In between, a mixing zone that has developed between

the fresh and saline groundwater separates the two, with the freshwater lens, here, defined as the groundwater with resistivity higher than 25 Ωm. The mixing zones between the freshwater lenses on top and the saline groundwater below vary between 1.5 - 4 m in thickness but are on average about 2 m thick.

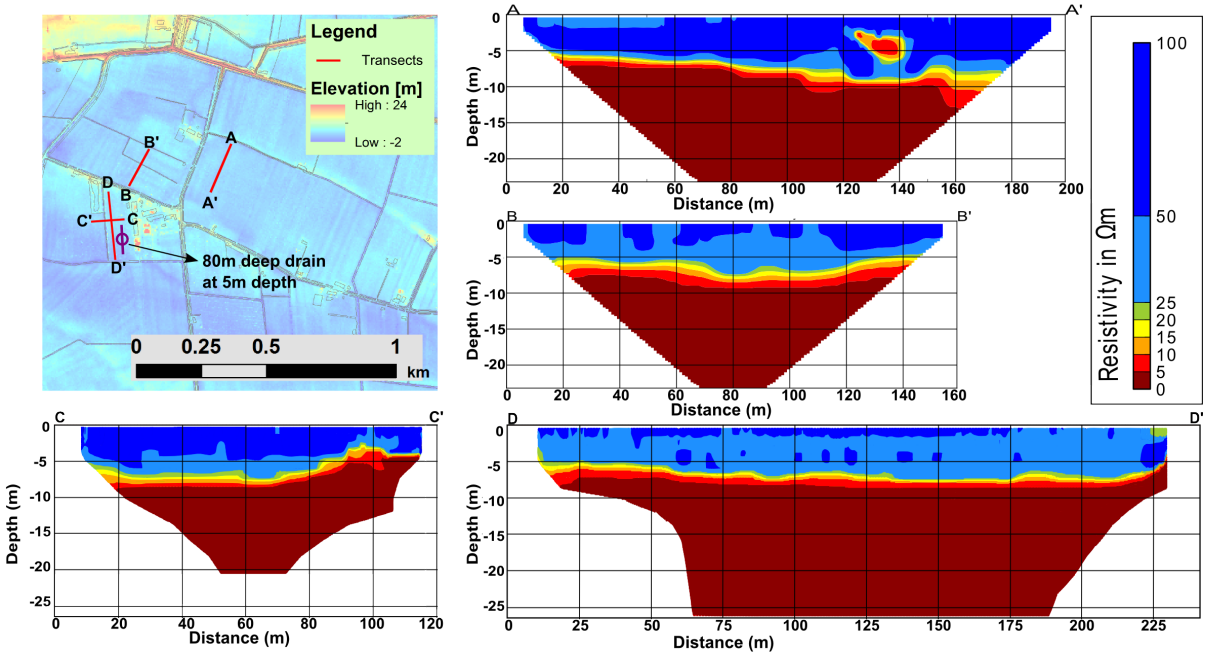

Figure 14: CVES profiles from the farmland of the Maljaars' and Korstanje. Profiles 'C - C and D' - D were made by Deltares in an initial field campaign. In the figure, Korstanje's deep drain (at 5 m depth) is indicated.

Profile A ($A - A'$), on the Maljaars' land, indicates a freshwater lens that is about 9 m at its deepest, in the center, and about 6 m at its shallowest, in the north (between 20 m and 40 m). Visible between distance 125 m and 145 m is a highly conductive body, thought to be a cable. This can be ignored and is most definitely not saline water. Profile B ($B - B'$) shows a freshwater lens with a depth of maximum 8 m and at the least, 5 m. This is in very good agreement with the EM-31 data, where a (very small) secondary ditch by (B') and a tertiary ditch by (B) appears to be the reason for some shallowing of the freshwater lens, likely due to some diffusive saline seepage. Profiles D ($D - D'$) and C ($C - C'$), also on Korstanje's land, and neighboring the deep drain used to pump 6000 m^3 of freshwater per year (mostly during summer), show very similar freshwater lenses. Profile D, shows a freshwater lens with a very consistent depth of about 8 m, and shallowing to 5 m in the North. Profile C also shows a majority of the freshwater lens being of about 8 m deep, shallowing to about 3 m towards the west, most likely due to the ditch the measurement crossed. Ditches are a common cause of upconing features of saline water as groundwater is able to move upwards due to the lower opposing groundwater pressure.

Korstanje's deep drain was installed in 1991, at a depth of 5 m, where measurements indicated a freshwater lens depth of 8 m. Since then, he has regularly used the deep drain to produce water for irrigation (primary use) and frost control. Only until recently (2011) has the deep drain produced slightly brackish water (. Seeing as the freshwater

lenses on the Maljaars' land and Korstanje's northern plot of land is also about 8 m in depth, there is certainly good potential for ASR, which would not only produce water, but also re-inject it.

8.2 Recommendations regarding saline seepage

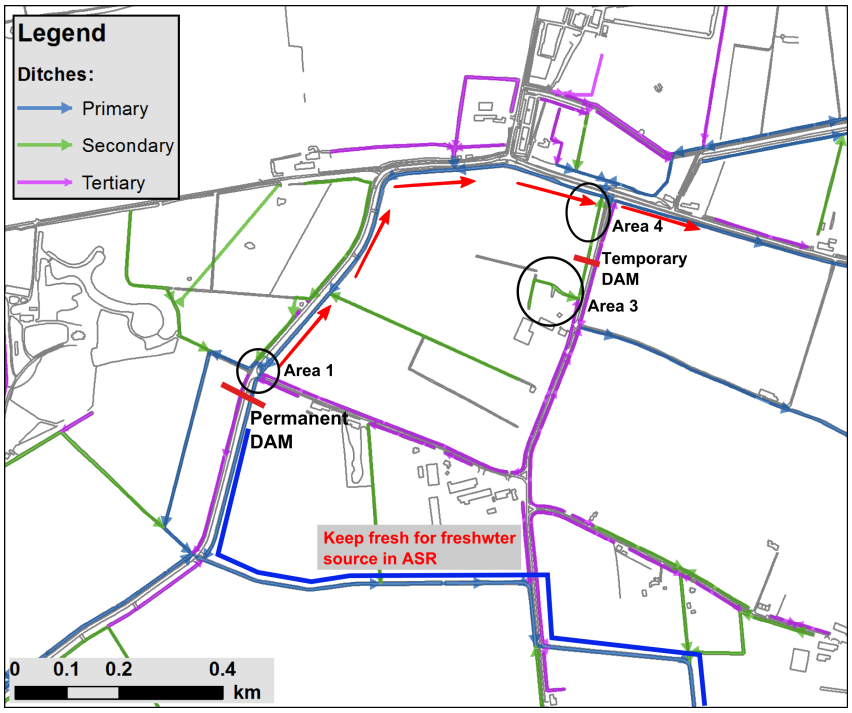

Figure 15: The locations for the placement of recommended dams and the location of saline seepage area 1, 3 and potential seepage location 4. Fresh ditches and new flow directions as a consequence of the building of the permanent dam is shown.

Recommendation 1 To determine whether or not are area 2 is an area of seepage, it would be recommended to place a temporary dam between area 1 and area 2 (see figure 15 for the location of the temporary dam). By isolating seepage area 1, and monitoring the ditch water downstream, in area 4 the Waterhouderij Walcheren could determine if there is a seepage source in area 2.

Recommendation 2 Overall , it would be ideal to separate the ditches prone to saline seepage as to keep the rest of the drainage system fresh and prevent further contamination of the farmlands to the south, see figure 15 for the location of the permanent dam. By placing a dam in the primary ditch, 100m south of the intersection where saline seepage area 1 is located, and forcing the water to flow backwards, following the red arrows in figure 15, to area 4 and continue east, across the junction , saltwater could be routed away from the area. This would keep the primary ditch fresh (labeled in figure 15), and likely assure freshwater in this ditch during winter, for use in aquifer storage. By re-routing the water to go north and leave eastwards, the Waterhouderij members to the south would

also have less chloride contamination and fresher ditches. An alternative would be to place a weir instead of a dam, as to maintain a higher ditch water level and keep the drainage direction. Higher ditch levels would put more pressure on infiltrating saltwater, with a likely benefit of reducing or even preventing seepage.

Recommendation 3 The most important recommendation based on the fieldwork data (and supported by modeling results, shown later), would be to close off or cover up the secondary ditch in area 3, in which saline seepage most certainly occurs (see figure 15). By burying the ditch with soil and allowing the groundwater level to rise in the area, saline seepage may be prevented. An alternative, and the easiest and cheapest measure would be to close off the ditch by a dam to prevent the spreading of the very saline waters.

8.3 Model hydraulic head results

In order to obtain a hydrological model which is representative of the current situation for the research area around Korstanje's and the Maljaars' land, it was necessary to create an equilibrium model, where, given initial condition of a completely salty system and the hydrological parameters necessary to model the system, the current situation could develop. We assumed that the current field situation is in equilibrium. By modeling the system for a long period, 100 years or more, we could observe how the model comes into equilibrium with the given stresses and input parameters. Upon reaching some state of equilibrium, where the model was not changing by a significant degree anymore over time, we compared it to the real situation, obtained from field observations, and try to validate the model. If significant differences were still observed, model calibration was conducted. By successively calibrating the model, we were able to come to a reasonably good representation of the field situation. This equilibrium model, or reference scenario, was then used to test scenarios of ASR.

Several steps were taken to obtain the equilibrium model or reference scenario. Firstly, an initial steady state head calibration was conducted to obtain the reference head distribution in the fields. This is important as heads drive flow which transports chloride. The assumption is that if the heads are correct, and the solute is conservative, then head driven flow will, if left to equilibrium, transport and disperse the chloride to the current chloride distribution found in the field. After head calibrations, salt runs were performed. Here, salt runs refer to long model runs allowed to attain equilibrium. This takes roughly 100 years and is further discussed below. For some head calibration points, field data was only available at depth, > 10 m, this meant that initial head calibrations had to be reanalyzed and adjusted for changes in chloride concentrations that were only obtained after the long salt runs. Chloride concentration effects the density of the groundwater which in turn effects the fictive freshwater head. At very shallow depths this effect is not that significant, but with depth this effect is intensified by the buoyancy term and can be very significant. So after the 100 year model runs and a change in the chloride concentrations, the modeled hydraulic heads change in relation to the chloride concentration changes. Model results show hydraulic heads decrease as a cell 'freshens' up. So initial hydraulic head calibrations had to estimate this change, and final hydraulic head calibrations must be performed during salt runs for the final equilibrium situation.

8.3.1 Model head calibration

Once the model parameters were defined, and the model built for MOCDENS3D, the first step was to calibrate the model and the model parameters based on fast, steady state model hydraulic head results. This is called the initial hydraulic head calibration. A total of 25 head calibration points were used to calibrate the model parameters. The location of the calibration points are shown in figure 16.

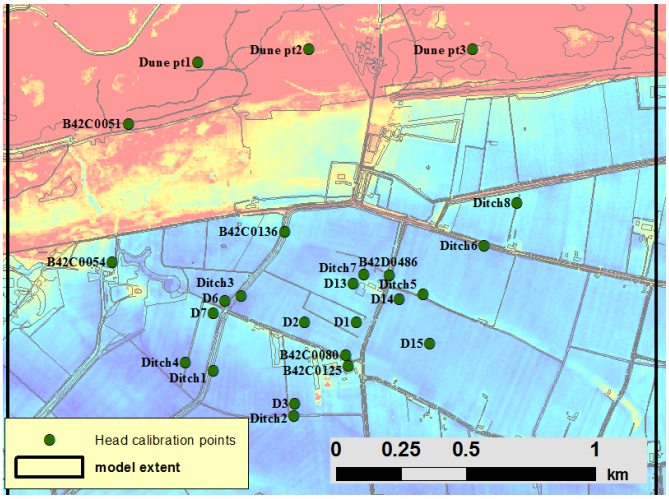

Figure 16: 25 head calibration points, where existing field data on hydraulic head could be used to calibrate the model.

The initial hydraulic head, model calibration, was conducted using the steady state option. By using the steady state option, MOCDENS3D calculates the 'steady state' or equilibrium solution (time derivative is equal to zero) for hydraulic heads based on all the stresses applied and the model parameters for each stress period. By using very small time intervals of a fraction of a day, for each stress period (summer and winter), model head calibration runs took a quarter of an hour. This allowed for necessary and frequent readjustments or calibration of model parameters and input stresses for the two different stress periods. This calibration procedure forms the basis for the long salt run calibrations that can take more than one week to run.

Figure 17 compares the heads from measurements in the field and model data for the final salt run calibration at 25 calibration points. Modeled head data is taken form model results of the final, transient, 100 year salt run at the end of summer and winter stress periods. This has accounted for density effects on freshwater head. Heads, measured in the field, are used to validate the model results. The dune and ditch calibration points show excellent agreement between modeled and observed hydraulic heads. These points generally show differences of only 10 cm or less.

Points D1 to D15 are shallow soil borings, conducted with a hand drill/corer. Groundwater levels reported here are based on high water and low water levels (in dutch abbreviated GHG and GLG respectively), derived form rust occurrence in the soil. Rust found among and coating the grains of the soil indicate groundwater fluctuations and can be used to derive the high and low levels of the groundwater. High levels are associated with winter, where groundwater levels are expected to be highest, and low levels with

summer. It is important to note here that these measurements record the widest groundwater fluctuations, hence this data represents extremely wet winters and extremely dry summers, and is not likely the norm in the field. Four of the eight 'D' points are missing data in summer because the low water levels were deeper than the hand drill could reach. These points are used for the purpose of knowing the upper and lower bounds of the groundwater fluctuations between summer and winter. The model should thus present groundwater levels below that of high waters in winter and above low waters in summer. This is in good agreement with field data. Point D7 in summer shows an unexpected discrepancy, where modeled heads are lower than the expected low water levels. Summer and winter ditch water levels in the vicinity of point D7 are -0.45 m and -0.65 m rel. to NAP respectively. One would thus expect that being so close to three ditches (< 40 m) the low water level would not be at 0.1m above NAP, and furthermore, looking at other differences between high and low water levels we see a typical difference of 1 m, and not 0.5 m. This head calibration data from the field is thus assumed to be too high and can be ignored for summer heads.

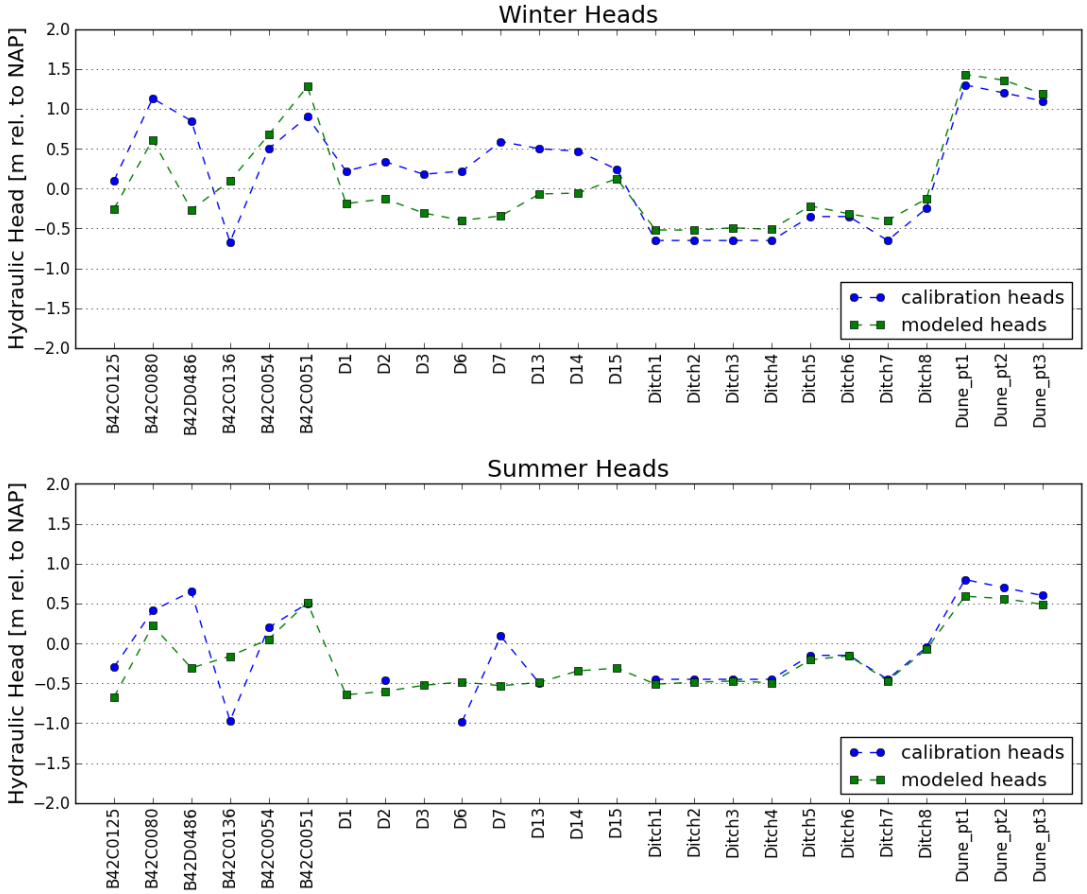

Figure 17: Final head calibration results using 25 calibration points (see figure 16), for summer and winter periods, based on model results and and field measured values for validation. 'Calibration heads' data is based on summer and winter yearly averaged measurements from the field. 'Modeled heads' data is taken form model results of the final, transient, 100 year model run (equilibrium or salt run) at the end of summer and winter stress periods. Hydraulic head data is all reported in fictive freshwater head.

Calibration points beginning with 'B' are wells or piezometers with hydraulic head data from the Dutch geological survey (TNO), available form DINO*Loket* (dinoloket.nl). Summer and winter field data is based on yearly averages of minimum and maximum heads (as expected at the end of the seasons) respectively. When comparing these calibration points to the modeled data, it is clear that some model results are very different from what is observed in the fields, namely points B42D0486 and B42C0136. A lot of work was put in to try and understand why there were these differences observed, when the rest of the model showed much better results. The main explanation for these differences is related to the piezometer proximity to ditches and the model horizontal resolution, 10 m $\times$ 10 m cells, which reports the head for one cell volume. Thus where the model calibration data point comes from a cell which has one or more ditches in it, the calculated heads are in a way the average situation in the cell domain, which can be very different from the piezometer reported head several meters form the ditches.

8.3.2 Final heads

The final heads in the surface cells for two stress periods, summer and winter are shown in figure 18.

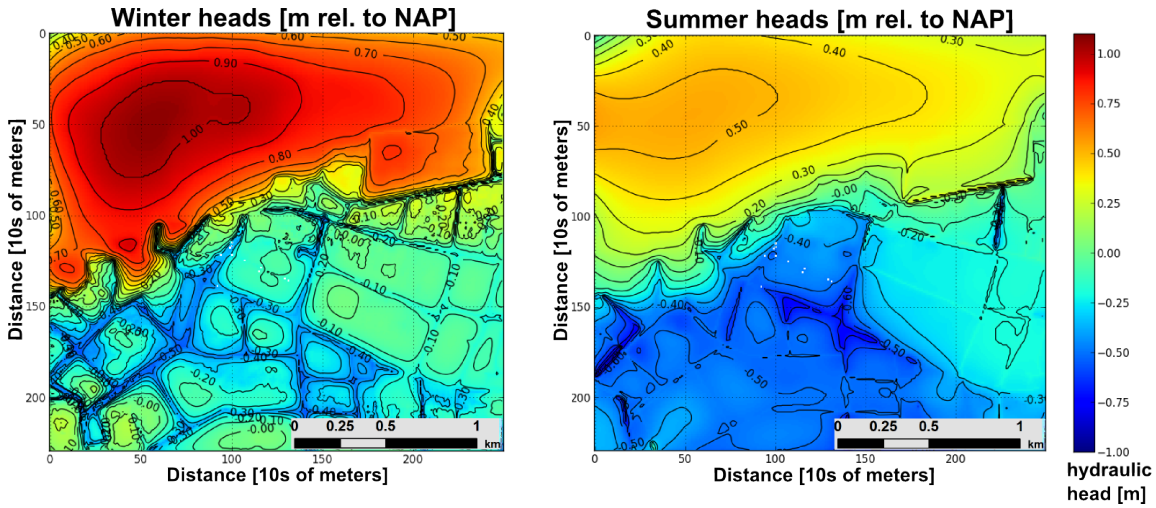

Figure 18: Final head (in m rel. to NAP) in the surface cells for the two stress periods, summer and winter. Contours are drawn for every 0.1 m.

Hydraulic head results nicely show the differences in summer and winter seasons. In winter, groundwater levels are higher due to a positive recharge flux. In the dunes, one can see the location of the water divide, which shifts slightly between the seasons. On the farmlands, groundwater levels are highest in the middle of the plots and lowest in the ditches, showing the net result of the drainage system. These heads are what drive recharge infiltration and one of the main forces in FWL formation.

8.4 MOCDENS3D investigations and error reduction

Initially, to gain a quick and dirty look at model concentration results, 100 year model runs were conducted under steady state flow, using one or eight particles. This gave a good

impression of how the model behaved and what was to be expected in final runs. Such runs took several days and produced several funny artifacts that were initially puzzling, but under investigation, gave rise to some important findings that have important implications in trying to reduce model error. These findings are of relevant interest to groundwater modelers and were further investigated for error reduction in this research.

8.4.1 Transient vs Steady State results

While making decisions for run parameters for salt runs, one of the decisions to be made was whether or not to run models under transient or steady state flow conditions. Steady state conditions have been explained above, effectively the time derivative of the advection dispersion equation is set to zero. Under transient conditions, heads readjust, over time steps, to the stresses applied to the model. Every stress period (summer and winter) is subdivided into monthly time steps, where heads are recalculated based on the applied stresses and time elapsed. Therefore, over one stress period, heads are recalculated every time step, allowing for a time dependent evolution of the heads. This has the effect of simulating a more accurate evolution of hydraulic heads and solute transport over time. Figure 19 shows model head and concentration results for transient and steady state flow. The model was run for 10 years from an initial situation of a completely saline system. The results shown are for a cell in the middle of Korstanje's Northern plot, 2.5 m below NAP.

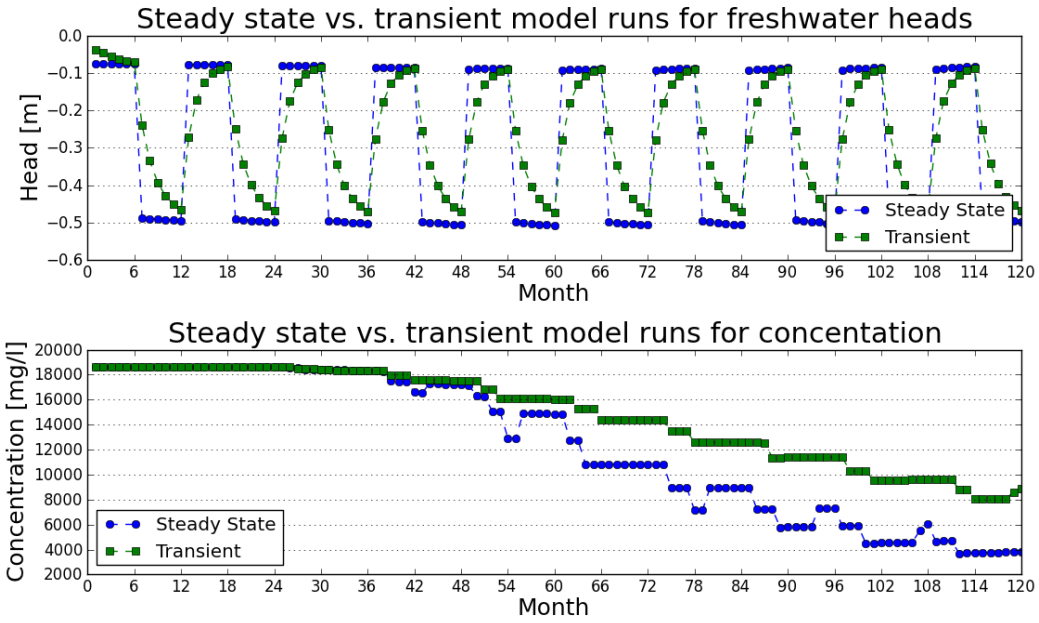

Figure 19: The effect of transient and steady state flow on head and concentration results for a 10 year model run starting with completely saline groundwater. Stress periods are six months (summer and winter) and time steps are one month, giving six time steps per stress period.

One can clearly see that for transient flow, where heads are recalculated every stress period, results show a much slower evolution of concentrations. The steady state chloride

concentrations decrease faster than transient concentrations (chloride is pushed downwards by precipitation) because over the six month winter stress periods (when recharge is positive), the heads are higher. Over long periods of time, steady state models (incorrectly) develop deeper freshwater lenses compared to transient models. This is illustrated in figure 20 for the same location on Korstanje's land. The figure however does not represent the same final calibrated model used as the reference situation. This investigation was carried out during calibration procedures and is illustrated here mainly to indicate that differences will occur.

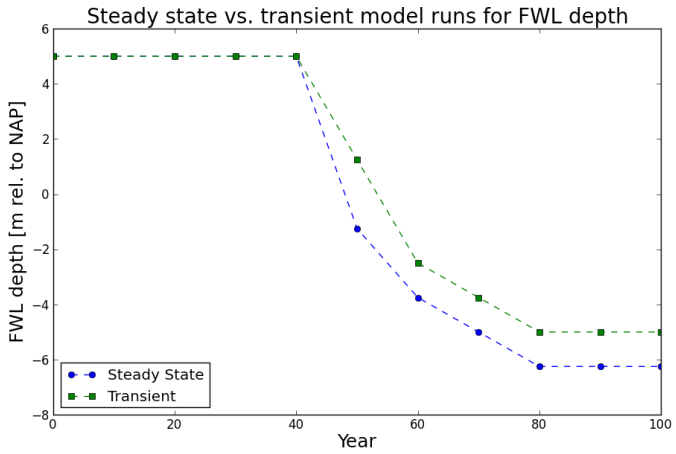

Figure 20: The effect of transient and steady state flow on freshwater lens depth for a 10 year model run starting with completely saline groundwater. Stress periods are six months and time steps are one month, giving six time steps per stress period. Note that this model run and investigation was not based on the final calibrated model, however they are very similar. It is mainly for the purpose of illustrating the fact that differences (or an error) in freshwater lens depth will occur (or be made).

Transient and steady state runs also have different calculation times. Transient model runs require significantly more time to run than steady state models. However, with respect to the errors made in solute transport and the evolution of freshwater lenses, for this modeling purpose, it was decided that transient runs would better simulate reality, especially when running scenario models, that have time steps of one week. Shorter time steps mean steady state approximation become more incorrect, as in the field, in a short time, hydraulic heads would most likely not reach equilibrium. Thus as discussed above, errors would be introduced. Therefore for this modeling study, despite the longer model run times, transient flow is used in the salt runs and the scenario runs.

8.4.2 Time to equilibrium situation

The time needed for the model to attain the equilibrium situation, or the (roughly) current field situation was determined by the time needed for the freshwater lenses to fully evolve and be in equilibrium with the model stresses and inputs. The freshwater lens development was used as an indicator as it is the slowest process and the most important for this modeling purpose. It was known that this equilibration time would be a long time, roughly 100 years or more.

Figure 21 shows the evolution of three different freshwater lenses on the Maljaars' and Korstanjes land, and in the dunes for a model run of 110 years. It is evident that after 110 yeas all freshwater lenses have reached some state of equilibrium. Here we assume the lens has reached equilibrium when the depth of the lens stops changing or is changing at a very small and insignificant rate. The FWL of the dunes is shown next to a decay curve with an asymptote of -34 m, of which the curve decays to. This is to illustrate that although the dune FWL is sill evolving (very) slightly, it follows a classical decay curve and will most likely stabilize at -34 m. As the lenses reached equilibrium in roughly 100 years, 100 years was deemed sufficiently long enough for model runs to attain equilibrium. Therefore, salt runs, are run 100 years before they were calibrated for chloride and FWL depth or used in scenario modeling.

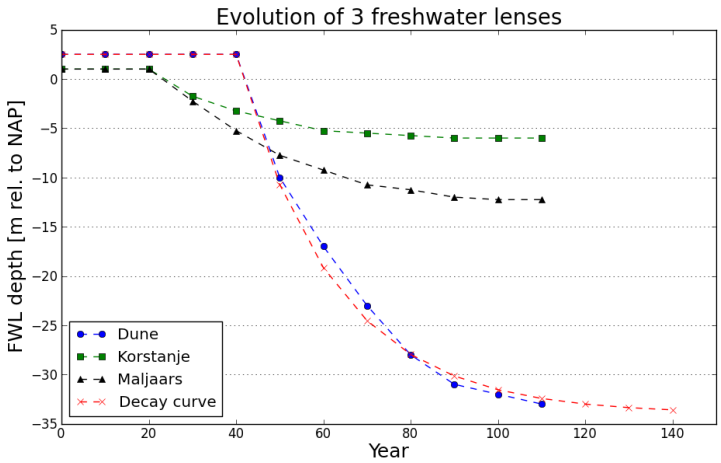

Figure 21: Time needed for three freshwater lenses to reach equilibrium and a comparison of the dune freshwater lens to a decay curve with decay rate, $\lambda = -0.045$ decaying to a value of -34 m, having the formula $Depth = 36.5e^{-0.045t} - 34$.

8.4.3 Choice of particles

MOC calculates the advection of solutes based on a particle tracking technique (methods of characteristics). A certain amount of particles are placed in each cell, these particles are advected by the calculated flow, and at the end of the transport step, MOC calculates the concentrations in each cell based on the amount of particles left in it. The more particles that MOC can use, the more accurate will be the overall calculation of the solute distribution. For a 64 bit processor, one can chose between 1, 8 or 27 particles. Using 27 particles will produce the most accurate results. As the choice of particles also effects the runtime of the model to a very significant degree, it was worth the time to investigate the effect of particle choice on model accuracy.

Figure 22 shows the differences in the evolution of two FWLs, in the dunes and a on the Maljaars' land. The use of one particle has clear inaccuracies. By using one particle, it is much harder to relate particle distribution to concentrations and MOC will make many numerical errors. With one particle, where flow may go up and down and sideways, only the main flow can be followed and mistakes are made because complicated advection

is poorly represented by this particle. With one particle, FWLs seem to stop growing at a certain point and all lenses develop to be much shallower than they should. Eight particles shows relatively good model performance as shown by figure 22. There are only slight differences in model results between 8 and 27 particles. Never the less, 27 particles shows the most accurate modeling results, however also requires the longest computation times. Therefore it was decided that for calibration runs, 8 particles would suffice to give a reasonably good model results and for final runs and scenario runs, 27 particles would be used. This allowed for faster model development at the calibration stage, saving up to two days in computation times.

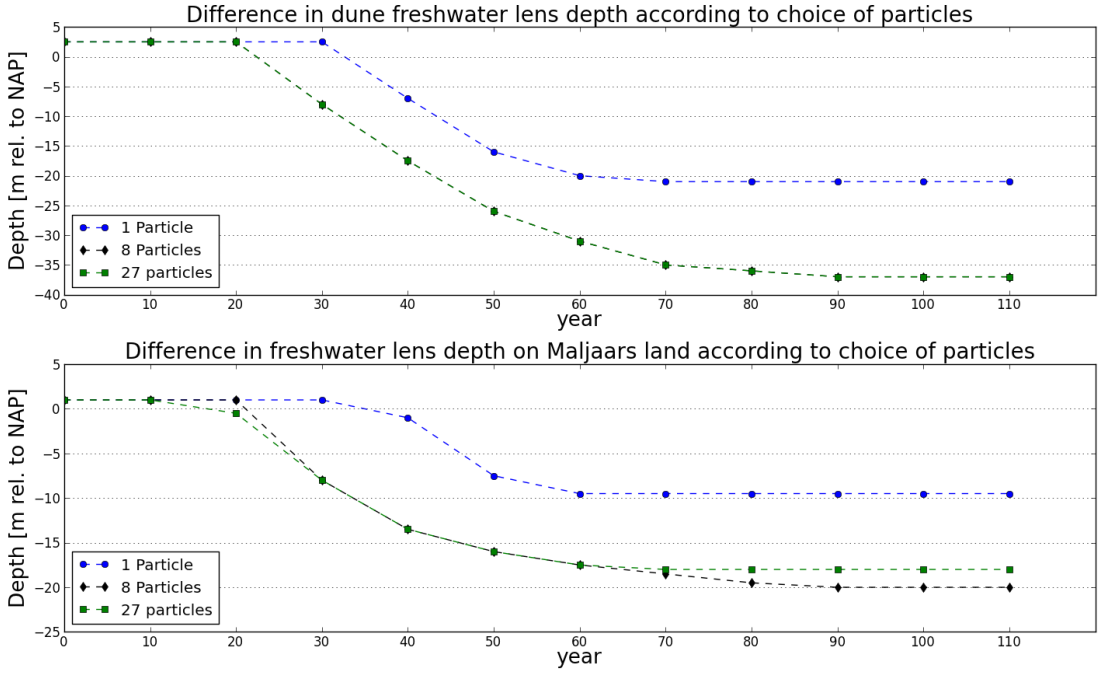

Figure 22: Modeled freshwater lens evolution in the Dunes and on the Maljaars' East plot of land over 110 years for a choice of 1, 8 and 27 particles.

8.5 Model chloride concentration results

Chloride concentration calibrations were based on the depth of the freshwater lenses obtained by CVES transects C and D and where possible the EM-31 results. Also some existing data of the freshwater lens in the dunes was used to calibrate the dune FWL depth. During calibrations, CVES transects A and B were not yet measured. Chloride concentration calibration was performed after the model was run for 100 years, the so called 'salt runs'. Calculating a salt run with 8 particles under transient flow took about 10 days on a 64bit server like work station dedicated for model computations. 16 GBs of memory was just enough to process and build the model for a 100 year run. Several model building tricks had to be employed to prevent memory crashes, such as manual (by python code) copy/pasting of large arrays together to build the large input files for MOCDENS3D. This meant that chloride calibration took a lot of time, and often, by trying to fix one inaccuracy, others developed. Because time was restricted for this

project, most chloride calibration time was spent trying to obtain reasonable results and understanding the model (as is needed to carry out calibrations).

8.5.1 Model chloride concentration calibration challenges

Depth of the dune freshwater lens Several serious model errors with respect to chloride concentrations arose. One of the first issues faced was the depth of the freshwater lens on the dunes. Using GHB cells in the Northern border with head and concentration values taken from the Zeeland model (*Van Baaren et al.*, 2011) gave a dune FWL that was too shallow. It was known form several piezometers in the dunes that the freshwater lens reached a depth of roughly 35 - 40 m in the West of the model domain. When the North boundary GHB cells were converted from the Zeeland model heads to a hydrostatic head distribution (as discussed in the methods section above), the dune FWL developed to what was expected, roughly 35 - 40 m. This is nicely visible in figure 24, where the dune FWL reaches a maximum of 38 m. Issues with building (sub) hydrological models based on data form regional models such as adopted in this research for the boundary conditions, are not uncommon. More research into these general issues associated with adopting boundary conditions form regional models to build (sub) models, and what the prerequisites are for successful adoption could seriously benefit fellow researchers and industry in the field of groundwater modeling. Although it may seem logical to adopt boundaries form larger models at natural boundaries such as water divides, rivers, etc. in reality, often groundwater modelers do not have this option due to restrictions of for example model size, or are faced with dynamic boundaries which may migrate back and forth in space like the dune water divide.

Excessive seepage and high velocities Another issue faced was the amount of seepage and high velocities caused by upward and downward flows in the cells below some ditches. This issue was often found to pertain to cells with multiple ditches, for example at junctions. Calculated ditch lengths and thus conductances for cells with multiple ditches was very high, allowing for high velocities and unnatural saline seepage fluxes, more than what was expected or observed. High velocities meant that MOC could only calculate transport with small transport time steps (as to maintain accuracy and reduce numerical errors) making model run times very long. In the beginning, run times were roughly two weeks. Manual adjustments to conductance values had to be made to decrease excessive seepage and high velocities in several 'troubled cells' with too high river conductances. A lot of work was put into calibrating the conductances of ditches, which provided to be very challenging. Smaller ditches, such as the tertiary and secondary ditches in the north and center of the model domain continue to still give inaccurate results for seepage fluxes. The method adopted form Deltares to calculate ditch conductances was reevaluated and adjusted, however more work into this area would have proved beneficial to final model results.

8.5.2 Model chloride concentration calibration using CVES transects

CVES profiles C and D (see figure 14) were used to calibrate the model salt run concentration results on the farmland. Transects taken form the model at the same location of

CVES transects A, B and D are shown in figure 23. Although transects A and B were not used during calibration, they are here compared and discussed for verification. Transects A and B were only obtained at the near end of the research, and could only be used in several last model calibrations, they are here compared and discussed, regardless. Transect C is left out as the area where the measurement was conducted is well represented by transect D.

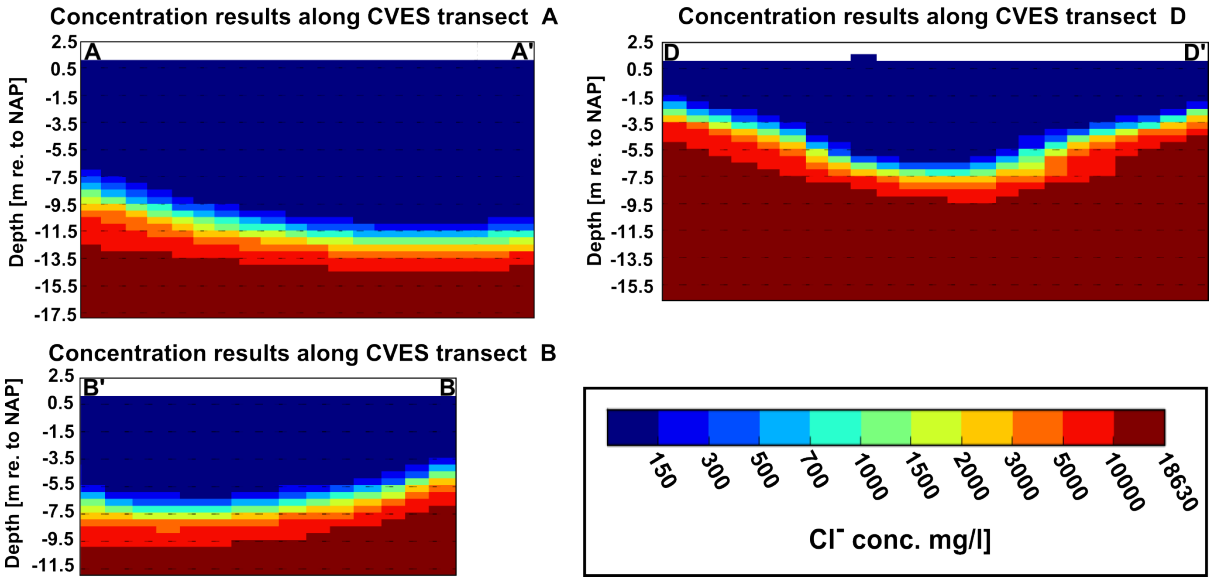

Figure 23: Modeled chloride concentration transects along three CVES transects (transects A, B and D). Calibration based on freshwater lens depth was performed using transects C and D.

Comparing CVES transect A with the modeled chloride results at the same location (figures 23 and 14 respectively), it is clear that the model predicts a FWL that is too deep, 12.5 m v.s. 9 m. This transect was not used during calibration. The results show some nice similarities, such as the depth of the FWL around A and the general deepening of the lens from A to A'. The mixing zone is modeled as being slightly larger, but there is good agreement in some locations. This plot of land does not use tile drainage as the other plots do because it naturally drained well and was never needed according to the farmers. It was also one of the main reasons why it was picked as a location to research ASR scenarios. The farmland plot likely has a higher horizontal conductivity than implemented in the model.

Comparing transects B, there is relatively good agreement, only that close to the ditch by B', the model predicts a lens that is 7 m deep and CVES measurements indicate a lens of only 5 m. Slightly more upconing of saline groundwater into the ditches is what one should see. In initial model results, the ditch bordering transect B, close to B' (dividing Korstanje's and the Maljaars' land) experienced too much saline seepage and upconing than what was expected form field observations. This small secondary ditch was then converted to a drain in the model, but this appears to attract less seepage. Reducing the drain resistance could improve model results. Close to B, the model transect shows a FWL that is 1 m too shallow. This is caused by the intense saline seepage and upconing in the ditch bordering B, and is further discussed in section 8.5.3. The mixing zones

between the two transects shows excellent agreement, both roughly 3 m thick.

Comparing transects D, there is very good agreement for the maximum FWL depth. The CVES transects carried out in the field indicate a FWL with a maximum depth of 8 m, equal to the the modeled maximum FWL depth. However, as with transect B, close to the ditch by D and D', model and field results show differences, with the modeled FWL becoming 2 meters too shallow by D and 2.5 m too shallow by D'. Like the results for transects A and B, the mixing zone simulated by the model is roughly 3 m. This is slightly thicker than what was found in the field from CVES measurements, roughly 2 m, reaching 3 m only in some locations.

Over all, on drained farmland, the model shows FWL depths that are in good agreement with field measured FWL depths. On the Maljaars's undrained plot of land, where transect A is, the model performance was slightly inaccurate, predicting a lens that was 3.5 m too deep. Model performance could be improved in this area by increasing the horizontal conductivities in the deklaag, thereby draining more recharge into the ditches instead of for FWL formation. Due to the long time required to run a salt run and thus conduct calibrations, not all model parameters could be optimally calibrated.

8.5.3 Final chloride concentration results

Figure 24 shows the final model concentration results at -2 m below NAP and the modeled FWL depths on the farm plots and in the dunes. The FWL depths are based on the depth to the interface (concentration = 300 mg/l). Concentration results are shown for a depth of 2 m below NAP, the approximate bottom of the top semi-confining unit, the *deklaag*, which is thought to be about 3 m thick in the area.

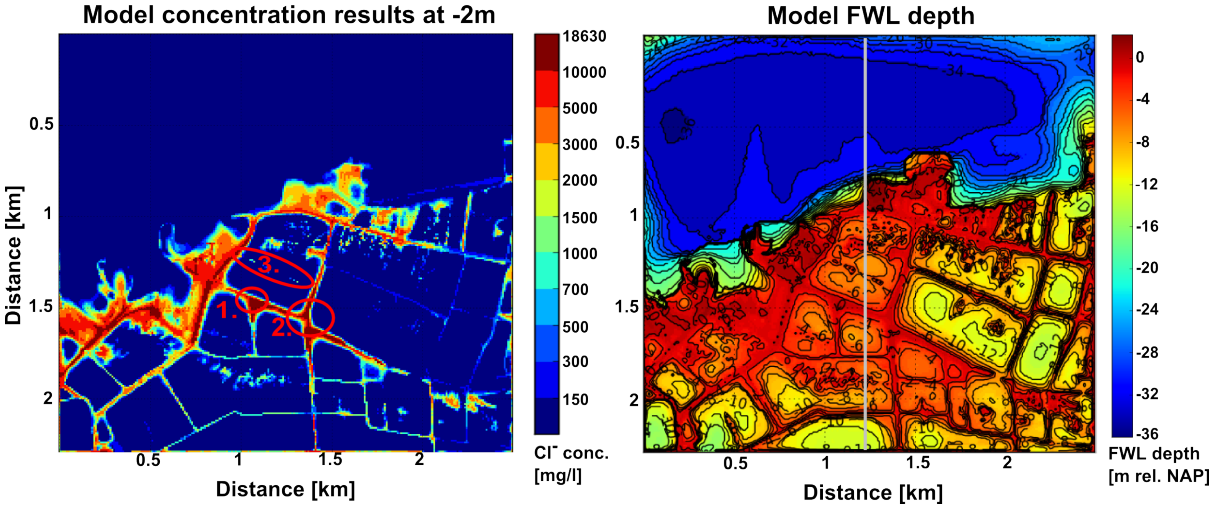

Figure 24: Model concentration results at -2 m below NAP (below *deklaag*) and modeled FWL depth (interface located at concentration = 300 mg/l). Also drawn in the location of the model chloride concentration results transect shown in figure 25.

The concentration results form -2 m below NAP show the model results of the simulated final saline seepage effects to the shallow subsurface. Studying these concentration results, one can see that there is good agreement between modeled data and the fieldwork data as described in the fieldwork results, section 8.1, e.g. EM-31, CVES, and

Cl^-concentrations. Most importantly, areas of possible seepage found from fieldwork are confirmed here in the model results (see section 8.1.4).

The most notable observations are that the ditches are a prime location for seepage. Furthermore, ditches around the center of the model, the interest area of Korstanjes and the Maljaars' farms, appear to be an area of that experiences more saline seepage relative to the surroundings. It should be noted that closer to the model boundaries it is expected that model results become more inaccurate and should not be used. Not all problematic areas could be calibrated for excessive seepage, but many measures were taken to try to make the model as realistic as possible. This even included introducing the most likely dry ditches in summer into the model. Information which was gathered with the help of the farmers and the local water board. Non the less, three ditches were very difficult to control for: (1) the ditch between Korstanje's two plots of land (marked with a circle and labled '1.' in figure 24). (2) The ditch intersection in the middle of the model terrain (marked with a circle and labled '2.'). And (3) the small ditch separating Korstanje's and the Maljaars' land (marked with a circle and labled '3.').

The first troubled area is in two tertiary ditches alongside a road that are hardly ever filled with drainage water. Sometimes during heavy rainfall in winter they act as drainage ditches. The model however indicates very high rates of seepage. This is not observed in the field. The same situation applies for the second troubled area, an area with many tertiary ditches, one bordering each side of the road and the two intersections. In the field, these ditches rarely act as drainage ditches, and show no saline seepage, but the model simulates a lot of seepage. It appears that the conductances of small tertiary ditches were modeled as being too high or the combined effect of several ditches in one model cell raised the conductance too much, allowing for excessive saline seepage to come through the ditch bottom.

The third area, a small secondary ditch as presented above, initially also suffered too much seepage. This ditch was converted to a drain, but resistance values were still too low as indicated by the shallower than measured upconing under the ditch by CVES fransect B. Although results are non the less relatively good, by increasing the conductances of these cells, or decreasing the drain resistance the seepage rates could be increased slightly. There was however not enough time to perfect the solution to fix these ditches. It should be noted however, that they are slightly incorrect.

Figure 25 shows a general schematization of the local hydrology based on model results in a N-S transect. Shown are the dune and farmland plot-sized FWLs and chloride intrusion from the sea, flowing under the dunes and into the shallow groundwater system as saline seepage (mainly into the ditches).

Modeling the whole area while trying to keep as many factors accurate, such as the dune FWL, and the individual lenses on all the plots of land around the center of the model, proved challenging in the time frame given. However it did allow for a better understanding of the hydrological system in general (see figure 25 for a general schematization of model results and chloride transport). Saline seepage is originating from intruding seawater that enters the system by flowing underneath the dune FWL. The dune FWL extends all the way up to the farmland plots, which is beyond the dune area (in the North portion of the model domain). Although this area has been given back to nature, water that drains out of the dunes is fresh and can be used for ASR so long as it does not mix with the saline seepage from the Maljaars' land.

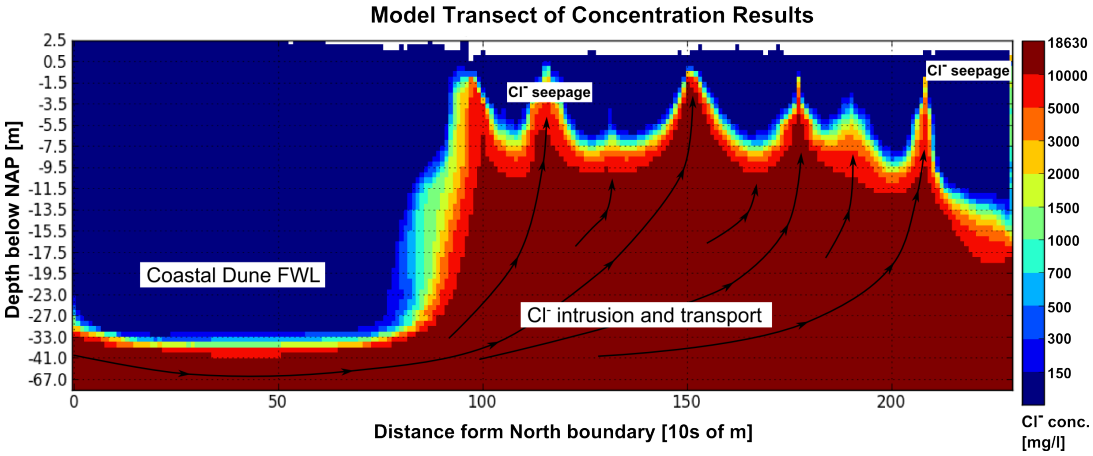

Figure 25: Model chloride concentration result transect showing general salt transport into the model domain and seepage into shallow groundwater system. Also visible are the dune and farmland plot-sized FWLs, fed form recharge. The location of the transect is shown in figure 24. Please note that the tick marks on the y-axis, showing the depth, represent larger differences with depth. This y-axis actually plots the different layers, (which have different thicknesses), the labels represent the depth of the centers of the many model layers.

There was a high correlation between deeper freshwater lenses and higher terrain or surface elevation, as this allowed for higher groundwater levels and thus larger FWLs. Between winter and summer the model showed, as suspected, that the freshwater lenses grow and contract slightly. Ditch water levels also had a large effect on the amount of seepage coming through. Higher ditch water levels as maintained in some ditches or during the beginning of summer generally suppresses saline seepage, and when water levels are low such as in winter or when ditches dry up, saline seepage strengthens. Overall, even though some inconsistencies are present, the model shows a very nice model of reality and is very well capable of modeling the hydrological processes found and expected in the field for a typical Dutch coastal setting.

8.6 Model scenario results

Three scenarios are modeled to determine their hydrological potential and feasibility to increase fresh water availability for the farmers in the area. Two of the scenarios are based on the use of a deep horizontal drain for ASR, where in winter freshwater water can be pumped into the subsurface FWL for storage and in summer the freshwater can be pumped out for irrigation. This ASR method is of interest to the local farmers, and a study to determine the feasibility is needed to ensure no disruptions and salinization of the FWL system occurs if the scenarios are undertaken. A third scenario is based on a newly proposed drainage scheme brought forth by the farmers, with the hope that it would reduce seepage. Table 7 gives a summary of the model results.

8.6.1 Scenario 1

The first scenario tested was the effect of artificial injection or recharge and production on the North farm plot of Korstanje. Infiltration was carried out through a 100 m deep drain at -5 m below ground level. The elevation is roughly 0.85 m rel to NAP. This setup is similar to what Korstanje has already used on his land to the South, however here we consider artificial recharge during winter and production during summer. To aid in the infiltration and storage of freshwater, ditch water levels were also increased by 0.2 m year round. 10000 m^3 of water is injected over six months of winter and 6000 m^3 is produced (extracted) steadily over six months of summer. This would supplement Korstanje's current deep drain and allow him to produce 12000 m^3 freshwater per year over the summer months. Figure 26 shows the results of ASR scenario 1 after five years of injection and production over winter and summer.

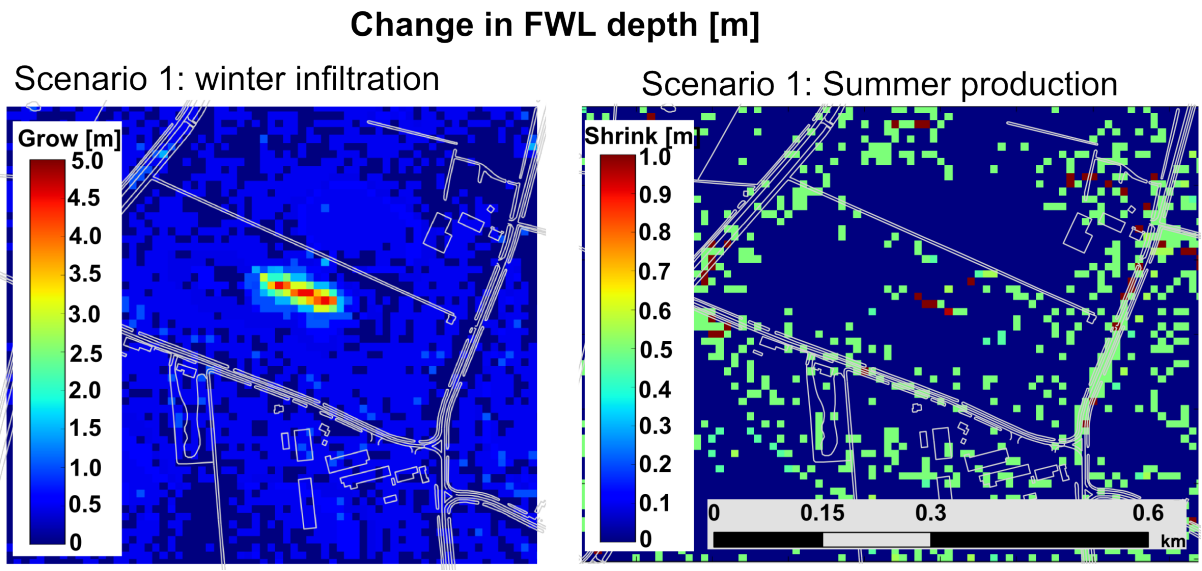

Figure 26: Scenario 1 results showing the growth and contraction of the freshwater lens relative to the equilibrium winter and summer months FWL sizes, respectively. All changes are reported after five years of repetitive ASR. Notice in the summer production figure, some shrinkage of 0.5 m is visible in the domain, this is due to seasonal contractions of the FWL and upward migration of the interface in some locations due to negative recharge, but can be ignored.

Results are shown for after five years. It was chosen to report results after five years to ensure no negative trends of salinization. Results show that injection of a total of 10000 m^3 of water over one winter results in a deepening of the freshwater lens of up to 4 m, with an influence area of 150 m $\times$ 80 m increasing in at least 1 m. Groundwater levels directly above the injection well increased by no more than 0.4 m compared to the equilibrium situation (reaching no higher than 0.60 m below ground level). Approximately 20 m from the groundwater (infiltration) bulge, the groundwater level returns to roughly the depth of the tile drains at -0.9 m below ground level. This is still safe for Korstanje's fruit trees and only poses a minimal threat of water damage to the roots in the direct vicinity of the deep drain.

At the end of summer, after extracting 6000 m^3 of freshwater, a maximum of 1 m of saltwater upconing was observed. Here the FWL (according to the model) is 8.5 m thick, meaning that no saline water entered the deep drain during production. This upconing relaxes and disappears again over the successive winters during injection. Groundwater levels at the end of summer pumping dropped no more than 0.05 m relative to the summer equilibrium situation. It is thought that this small, almost negligible, change in the summer groundwater levels is due to the 0.2 m increase of ditch water levels which acts to support higher groundwater levels. This poses no significant stress to Korstanje's fruit trees and their roots as water fluctuations are kept at a minimum.

This scheme is sustainable over the years and is a viable way to produce water for farmers who do not have direct access to a fossil sandy creek bed, which can make a far more ideal ASR location due higher conductivities (*Visser*, 2012).

8.6.2 Scenario 2

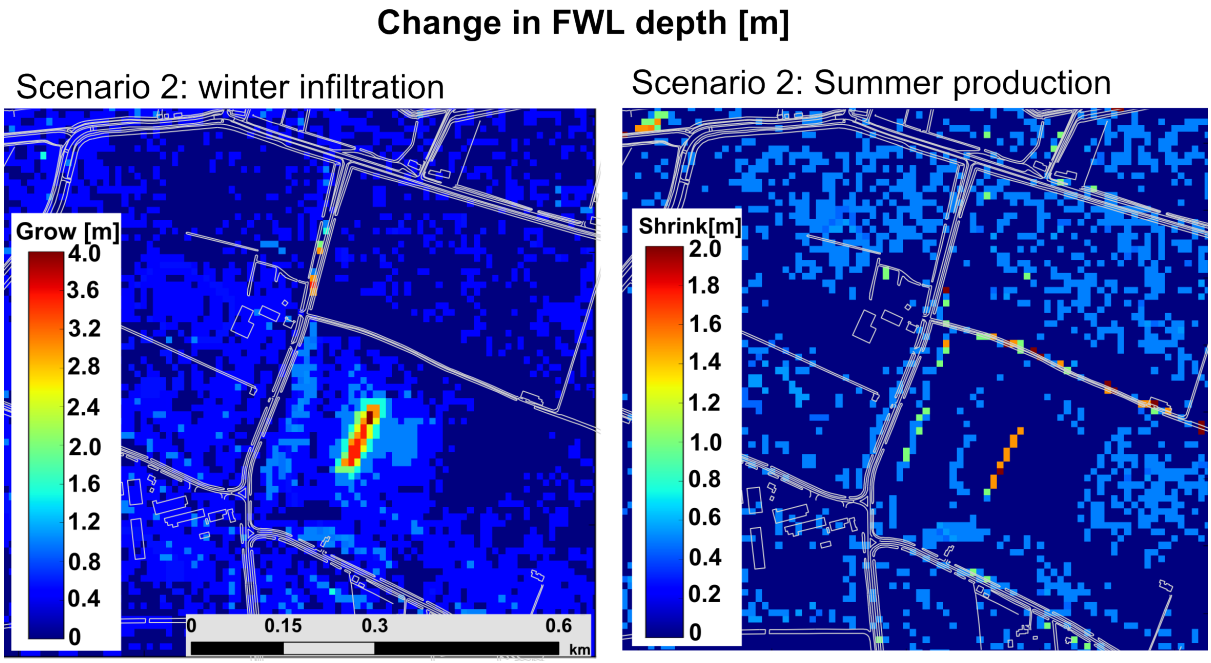

Figure 27: Scenario 2 results showing the growth and contraction of the freshwater lens relative to the equilibrium winter and summer months FWL sizes, respectively. All changes are reported after five years of repetitive ASR. Notice in the summer production figure, some shrinkage of 0.5 m is visible in the domain, this is due to seasonal contractions of the FWL and upward migration of the interface in some locations due to negative recharge, but can be ignored.

The second scenario tested was almost identical to the first, however located on the farmland of the Maljaars where there is no drainage and at a different depth. It was hoped that this would produce more interesting results as infiltration is not lost to drainage. The elevation of the land is roughly 0.9 m rel. to NAP. Infiltration was carried out through a 100 m deep drain at -9 m below ground level. 10000 m^3 of water is injected over six months of winter and 6000 m^3 is produced steadily over six months of summer. To aid

in the infiltration and storage of freshwater, ditch water levels were also increased by 0.2 m year round. Figure 27 shows the results of ASR scenario 1 after five years of injection and production over winter and summer.

Results are very similar to scenario 1 above, however as expected (due to no tile drainage) the FWL grew larger for the same injection. Results show that after winter injections of 10000 m^3 of freshwater, the FWL grew a maximum of 4 m, with an influence area of almost 200 m $\times$ 200 m, increasing by at least 1 m. This is significantly larger than the results on Korstanjes land. Relative to the winter equilibrium situation, groundwater levels directly above the injection well increased by no more than 0.25 m (reaching no higher than 0.65 m below ground level). This groundwater (infiltration) bulge diminishes within a larger distance from the drain, compared to scenario 1, roughly 30 m, however, there being no winter crops here in winter, the deepening of the groundwater below the surface poses no threat.

At the end of summers, when 6000m^3 of freshwater had been extracted, there was an upconing of 1.5 m, but the water reaching the deep drain is still fresh. Here the FWL (according to the model) is 12.5 m thick, meaning that no saline water entered the deep drain during production. This upconing relaxes and disappears again over the successive winters during injection. Directly above the deep drain, groundwater levels at the end of summer pumping showed a slight increase, of at most 0.05 m relative to the summer equilibrium situation (to roughly -0.2 m rel. to NAP). Further away from the deep drain and closer to the ditches, the groundwater level increase reaches its maximum, of roughly 0.15 m. This small increase in summer groundwater levels is supported by the increased ditch water levels and could have a slight positive effect on crops. The current summer groundwater table (roughly -1.3 m to -1.5 m below ground level) is slightly low compared to the average field situation, a small increase would likely benefit the crops.

This ASR scheme has tested to be a sustainable and yearly-wise reproducible, capable of producing much needed freshwater for the farmers who are located in this relatively salty area. Should The Maljaars' chose to implement such ASR in this plot of land, it would be advisable to locate the deep drain slightly more shallow to ensure no upconing of saline water. Around 7 m below the ground level would be ideal.

8.6.3 Scenario 3

Farmers of the Waterhouderij Walcheren wanted to know the possible effect of a change in the drainage levels on the surface water salinization or saltwater intrusion and the freshwater system. A new drainage scheme, of different ditch water levels throughout the year, was drafted by the farmers for implementation in and study by this model. Table 6 shows the new drainage scheme that was implemented and figure 28 shows the model results to the surface freshwater system.

Model results showed that under the new drainage scheme freshwater lenses neither grew nor contracted by any significant amount. Some lenses grew or contracted by a maximum of 0.5 m, but as natural recharge fluctuations are the main cause for such fluctuations of this magnitude, these results were termed insignificant. Never the less results to the surface water system, as indicated by salinization of ditches showed significant results. Looking at figure 28 one can easily compare the equilibrium or reference model results and the scenario results in relation to the surface water chlorinity. It is evident

Table 6: New drainage scheme as proposed by the farmers of the Waterhouderij Walcheren. The scheme involves changing the ditch drainage levels with hope that it will help promote a fresher surface water system and larger FWLs.

Month	Old drainage level	Drainage level under new scheme
January	winterpeil	winterpeil +0.2 m
February	winterpeil	winterpeil +0.2 m
March	winterpeil	winterpeil +0.2 m
April	zomerpeil	zomerpeil +0.2 m
may	zomerpeil	zomerpeil +0.2 m
June	zomerpeil	zomerpeil +0.2 m
July	zomerpeil	zomerpeil +0.2 m
August	zomerpeil	zomerpeil −0.1 m
September	zomerpeil	winterpeil
October	winterpeil	winterpeil
November	winterpeil	winterpeil
December	winterpeil	winterpeil

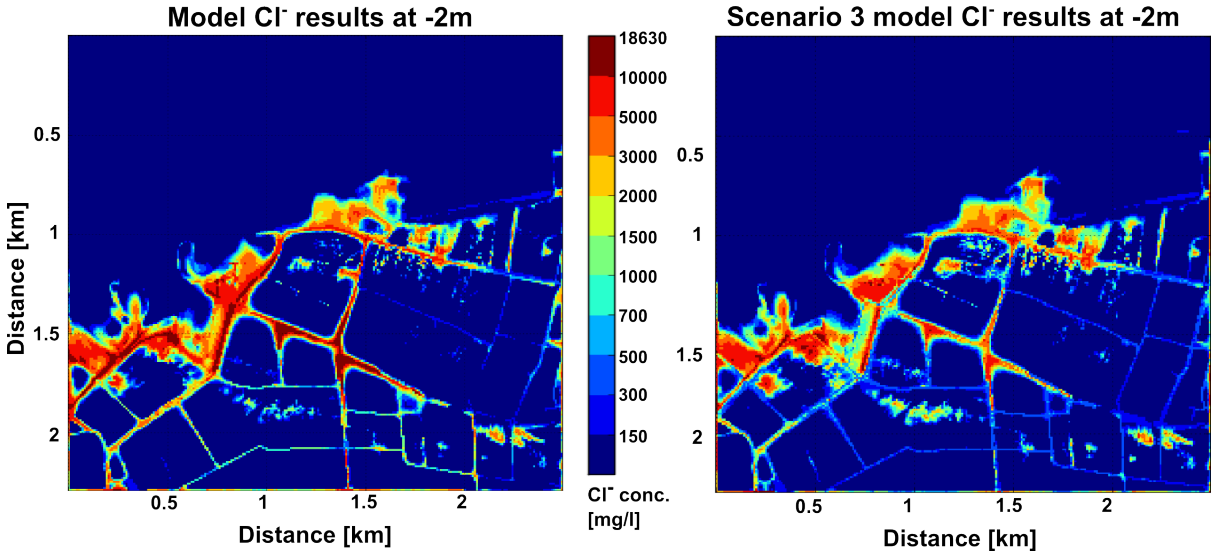

Figure 28: Model chloride results at 2 m below NAP taken form the equilibrium or reference model (for comparison) and scenario 3 results showing changes in surface salinization from seepage. Changes are reported after five years of adapting the new drainage scheme.

that the amount of seepage into the ditches has decrease, as shown by lower ditch water concentrations in many areas. This is due to the greater countering pressure of the higher ditch water levels on the upward flowing saline groundwater. However also evident is that the seepage areas outside the ditches have expanded. This is due to an increase of more diffusive like seepage underneath the farmland plots instead of concentrated seepage in the ditches. So although this new scheme appears to suppress saline seepage into the ditches, it could also be the cause for the spreading out and increase of seepage on land.

Having the option to rout away the saline water which preferentially seeps up in the ditches, would be ideal compared to having more land contaminated by seepage. It would be advisable then that a new routing scheme, as discussed in the field results section, be used to rid of saline seepage in the area.

Table 7: Summary of scenario results

Scenario	**Actions**	**Effects**
Scenario 1 (Korstanje)	- Infiltration through 100 m deep drain - At -5 m below ground level - Of 10000 m^3 of water injected over winter - 6000 m^3 extracted over summer - Ditch water levels increased by 0.2 m year round	Infiltration caused: - Deepening of the freshwater lens of up to 4 m - Groundwater level increase of max 0.4 m Extraction caused: - Maximum 1 m upconing - Groundwater levels dropped by a max. of 0.05 m
Scenario 2 (Maljaars)	- Infiltration through 100 m deep drain - At -9 m below ground level - Of 10000 m^3 of water injected over winter - 6000 m^3 extracted over summer - Ditch water levels increased by 0.2 m year round	Infiltration caused: - Deepening of the freshwater lens of up to 4 m - Groundwater level increase of max 0.25 m Extraction caused: - Maximum 1.5 m upconing - Groundwater levels increased by a max. of 0.05 m
Scenario 3 (entire model)	- New ditch drainage scheme (see table 6	- FWL on farmland showed no significant change - Seepage into ditches decreased - Seepage areas outside ditches intensified

8.7 Model Uncertainties

Besides some of the uncertainties discussed and touched upon throughout the paper, many other uncertainties in and limitations to this model exist.

Hydraulic conductivity One of the largest and most important uncertainty present in this model is the hydraulic conductivity of the subsurface. A vertical hydraulic conductivity model was provided by the Dutch Geological Survey (TNO). This model was based on the mean results of 50 realizations for hydraulic conductivity. The main purpose of this model was for use in regional hydrological model such as the Zeeland model (*Van Baaren et al.*, 2011). For smaller, local hydrological models as this one, this conductivity model provided many uncertainties and several corrections had to be performed. Firstly, interpolation form 100 m cells to 10 m cells in the horizontal, were performed to reduce numerical errors in flow and transport, then manual adjustments of the conductivity model was performed. The conductivities, although based on real field data, was obtained between 1900 and present, and the product of interpolations. This meant that on a regional scale the conductivity model performed well, however on a smaller scale, many local inconsistencies were clearly evident. These inconsistencies were spotted based on an array of numerical artifacts found in modeling results during calibration runs and manual overviews of the data provided. Although manual adjustments proved to improve results, it further adds uncertainties. Also, as the conductivity data was based on vertical wells, there was a lot of vertical conductivity artifacts. In several areas of the model, there appeared to be vertical conductivity trends (high vertical isotropy) rather than horizontal, as implied by the natural layering of the different strata. These chimneys like structures provided many strange modeling artifacts and had to be removed. The ratio between vertical to horizontal conductivities was another uncertainty that was introduced and many calibration runs were performed to try to chose the best ratio. Lastly, surface conductivities and the conductivities of deep formations ($>$ 60 m below NAP) as well as those in the dunes also showed many unrealistically small or large values that had to be adjusted. Especially low surface conductivities which created large head bulges and unrealistically large freshwater lenses.

Dune FWL and boundary conditions The freshwater lens development in the dunes was one of the most time consuming model calibrations. In fact several groundwater modelers in the Deltares work group have had similar difficulties with dune FWL modeling. Problems pertained to the choice of vertical and horizontal conductivities as well as boundary conditions. Good results were obtained when a change form the regional Zeeland model hydraulic heads and concentrations at the North boundary to hydrostatic heads and manual setting of concentrations based on the expected size of the dune FWL was made. The switch to hydrostatic heads however, disregarded any vertical flow components in the model boundary. This simplification is of course incorrect, however the model did preform better and vertical flow non the less was observed in cells bordering the boundary. Further research into successful implementation of boundary conditions in dunes as well as what approach is best in choosing boundary conditions and values when building sub-models would prove beneficial for groundwater modelers doing similar research.

Model boundary results Because the size of the domain was somewhat between a regional and a local hydrological model some uncertainties arose pertaining to this. Using the Zeeland model heads (which had to be interpolated as well) at the model boundaries meant that inaccuracies in regional flows and at model boundaries were inherited. Furthermore, assigning seawater values for boundary cells added inaccuracies as the model depends on density as well. Therefore, around the model boundaries, inaccuracies are very likely and results should be interpreted with caution. Due to the large distance form the boundaries to the interest area however, it is assumed that these errors will not propagate to and effect the results in the area of interest.

Field equilibrium situation One of the important assumptions made about the field situation is that it is in equilibrium. Of course, it is difficult to determine the validity of this assumption, but it is a common assumption made in such modeling practices. For the purpose of the size of the smaller freshwater lenses on the fields, it is relatively safe assumption. But for the large FWL of the dunes, especially with the increasing pressure form the sea due to sea level rise, this assumption introduces some small uncertainties and errors.

Modeling As the results of modeling is very much dependent on calibration processes it is important to note that modeling as a whole is merely an act of trying to represent reality. One cannot take the results of such a model as fact, but rater as suggestive information or some form of informed possibility. Trends that models suggest are more accurate than exact values and where there is little data to validate a mode, errors can easily be made or overlooked. One example worth mentioning here with this model is the depth of the FWL along CVES transect A, where without calibration data, it was assumed that in the absence of tile drainage, a FWL of roughly 12.5 m was acceptable. Only after going back to the field and conducting another CVES measurement, was it clear that the model results were off the mark by 3.5 m.

9 Conclusions

Farmers in the Waterhouderij Walcheren are facing increasing issues of groundwater salinization and freshwater deficits in dry summer months. An investigation into the shallow groundwater system of the dune area between Ostkapelle and Vrouwenpolder and on the farmland plots of Piet Korstanje and the Maljaars' family was carried out to gain a better understanding of the freshwater and saltwater hydrology using geophysical methods and a modeling study.

The study location is that of a typical dutch coastal area. Coastal dunes sustain a freshwater lens that reaches a depth of not more than 40 m. Low lying farmlands behind the dunes are prone to saline seepage from the the underlying salty groundwater due to positive pressure differences form the sea. Farmland plots, sustain small plot sized freshwater lenses that are prone to seasonal variations. Geophysical measurements results of EC, T-EC probe chloride profiles and EM-31 conductivities from the field show saline water preferentially seeps up in ditches where the groundwater table is lowest. Saline ditches and three likely locations of seepage could be identified (see figure 13) and it is

advised that the saline water be routed away form the interest area towards the East so as to ensure several ditches remain fresh for aquifer freshwater storage and recovery. CVES measurement transects on the farmlands of Korstanje and the Maljaars' reveal freshwater lenses of no average between 6 m and 8 m deep. These lenses have potential for ASR purposes to store excess water during winter months, for use in summer, where water shortages often occur.

A density dependent groundwater flow model was constructed for the numerical transport code MOCDENS3D. The model was designed for the purpose of gaining a better understanding of the local hydrology and to test the feasibility of ASR scenarios to increase freshwater availability, as well as a proposed new ditch drainage level scheme to prevent salinization.

Two ASR scenarios, one on the northern farmland plot of Korstanje and the other on the Eastern farmland plot of the Maljaars', were successfully modeled and studied. Results of both scenarios are very similar and indicate that an injection of 10000 m^3 of freshwater over six months in winter and an abstraction of 6000 m^3 of water in summer is sustainable over long periods of time and does not cause further salinization. In summer the FWL grew a maximum of 4 m, with an influence area of 150 m $\times$ 80 m on Korstanjes land and almost 200 m $\times$ 200 m on the Maljaars' land increasing by at least 1 m. At the end of summer after every abstraction phase, there is slight upconing of the FWL (not more than 1.5 m), however this does not reach the abstraction drain. This upconing relaxes and disappears again over the successive winters during injection. Furthermore, the small groundwater level fluctuations observed due to injection and pumping showed no added threat to the fruit trees of Korstanje or the crops on the Maljaars' land. The ASR schemes that were modeled, proved to be sustainable and yearly-wise reproducible, capable of producing much needed freshwater for farmers who are located in this relatively salty area.

The modeling scenario study on the newly proposed drainage ditch water levels, proposed by the farmers, showed that no significant change was observable to the depths of the FWLs on the individual plots, however there was a marked reduction of seepage and chloride concentrations in the ditches due to the increase in ditch drainage levels. This however had the effect to increase more diffusive like seepage on the farmland plots, where it was observed that farmland seepage areas and chloride concentrations increased.

References

Aiken, G. R., and E. L. Kuniansky (Eds.) (2002), *U.S. Geological Survey Artificial Recharge Workshop Proceedings*, USGS, Sacramento, California, open-file report.

Badon Ghyben, W. (1888), Nota in verband met de voorgenomen putboring nabij Amsterdam, *Tijdschrift van het Koninklijk Instituut vor Ingenieurs*, *5*, 8–22, in Dutch.

Bear, J. (1972), *Dynamics of fluids in porous media*, Dover Publicaions, New York.

De Louw, P. G. B., G. H. P. O. Essink, P. Stuyfzand, and S. E. A. T. M. van der Zee (2010), Upward groundwater flow in boils as the dominant mechanism of salinization in deep polders, the Netherlands, *Journal of Hydrology*, *394*, 494–506, doi: 10.1016/j.jhydrol.2010.10.009.

De Louw, P. G. B., S. Eeman, B. Siemon, B. R. Voortman, J. Gunnink, E. S. van Baaren, and G. H. P. Oude Essink (2011), Shallow rainwater lenses in deltaic areas with saline seepage, *Hydrology and Earth System Sciences*, *15*, 3659–3678, doi:10.5194/hess-15-3659-2011.

Eduardo López Moreno, G. M., Oyebanji Oyeyinka (2008), State of the worlds cities 2010/2011, *Report*, UN-HABITAT.

Eeman, S., A. Leijnse, P. Raats, and S. van der Zee (2011), Analysis of the thickness of a freshwater lens and of the transition zone between this lens and upwelling saline water, *Advances in Water Resources*, doi:10.1016/j.advwateres.2010.12.001, in press.

Fitts, C. R. (2002), *Groundwater Science*, Academic Press.

Goes, B., G. H. Oude Essink, R. Vernes, and F. Sergi (2009), Estimating the depth of fresh and brackish groundwater in a predominantly saline region using geophysical and hydrological methoods, Zeeland, the Netherlands, *Near Surface Geophysics*, *7*, 401–412.

Herzberg, A. (1901), Die Wassesversorgung einiger Nordseebaden, *Zeitung fur Gasbeleuchtung und Wassesversorgung*, *44*, 815–819 and 842–844, in Dutch.

Igboekwe, M., and A. Ruth (2011), Groundwater recharge through infiltration process: A case study of Umudike, Southeastern Nigeria, *Journal of Water Resources and Protection*, *3*, 295–299.

Konikow, L., D. Goode, and G. Hornberger (1996), A three-dimensional method-of-characteristics solute-transport model (MOC3D), *Water-Resources Investigations Report 96-4267*, U.S.G.S., 87pp.

Lebbe, L. (1999), Parameter identification in fresh-saltwater flow based on borehole resistivities and freshwater head data, *Advances in Water Resources*, *22*, 791–806, doi: 10.1016/S0309-1708(98)00054-2.

McDonald, M., and A. Harbaugh (1988), A modular three-dimensional finite-difference ground-water flow model, *U.S.G.S. Techniques of Water-Resources Investigations*, book 6, Chapter A1, 586pp.

Oude Essink, G. (1998), Moc3d adapted to ismulate 3d density dependent groundwaer flow, pp. 291–303, MODFLOW'98 conference, Golden, Colorado, USA.

Oude Essink, G. H. (2001), Saltwater intrusion in 3D large-scale aquifers: A Dutch case, *Physics and Chemistry of the Earth (B)*, *26*(4), 137–158.

Oude Essink, G. H. (2011), *Density Dependent Groundwater Flow*, UNESCO-IHE Institute for Water Education.

Oude Essink, G. H., E. van Baaren, and P. De Louw (2010), Effects of climate change on coastal roundwter systems: a modelling study in the Netherlands, *Water Resources Research*, *46*, doi:10.1029/2009WR008719.

Post, V., and E. Abarca (2010), Saltwater and freshwater interactions in coastal aquifers, *Hydrogeology Journal*, *18*, 1–4, doi:10.1007/s10040-009-0561-9.

Post, V., H. van der Plicht, and H. A. J. Meijer (2003), The origin of brackish and saline groundwater in the coastal area of the Netherlands, *Netherlands Journal of Geoscience*, *82*(3), 133–147.

Post, V., H. Kooi, and C. Simmons (2010), Using hydraulic head measurements in variable-density ground water flow analyses, *Ground Water*, *45*(6), 664 – 671, doi: 10.1111/j.1745-6584.2007.00339.x.

Stuyfzand, P. (1993), Hydrochemistry and hydrology of the coastal dune area of the Western Netherlands, P.h.D thesis, Vrije University Amsterdam, Amsterdam.

Stuyfzand, P. (2009), Fresh water supply and water quality at national and regional scale, *Proposal: Adaptation to climate change*, Knowledge for Climate, in Work package number 4: Water technology as a tool box for self-sufficient regional water supply.

Stuyfzand, P., and A. Doomen (2004), The Dutch experience with managed aquifer recharge and storage: a review of facilities, techniques and tools, *Report*, Kiwa N.V./ NWP, Nieuwegein, the Netherlands.

Stuyfzand, P., and R. Stuurman (1994), Recognition and genesis of various brackish to haypersaline groundwaters in the Neterlands, 13, pp. 125–136, Salt Water Intrusion Meeting, University of Calgari , Sardinia.

TNO (1992), Inleiding in geofysisch boorgatmeten, een praktische cursus voor grondwater onderzoek, *Report*, TNO.

U.N. (1994), United Nations, Department of Public Information, New York.

Van Baaren, E. S. (2012), Presentatie overzicht waterhouderij walcheren, available at www.waterhouderij.nl.

Van Baaren, E. S., G. H. P. Oude Essink, P. G. B. G.M.C.M. Jaanssen, De Louw, R. Heerdink, and B. Goes (2011), Freshening/salinization of phreatic groundwater in the province of Zeeland: results of a 3-D density dependent groundwater model, *Report*, Deltares.

Van de Plassche, O. (1982), Sea-level change and water level movements in the Neterlands during the holocene, *Mededelingen Rijks Geologische Dienst*, *36*(1), 93pp.

Van der Meij, J. (1999), Modelling of the effect of sea-level rise and land subsidence on the evolution of the groundwater density in the subsoil of the northern part of the Netherlands, *Journal of Hydrology*, *226*(3-4), 152–166.

Van der Straat, A. (1986), Kreekruggen, *report*, Provinciale Waterstaat Zeeland, Middelburg, Zeeland.

Van Meerten, J. J. (1986), Kunstmatige infiltratie in kreekruggen, M.S.c thesis, Delft University of Technology, Delft.

Van Meir, N. (2001), Density-dependent groundwater flow: Design of a parameter identification test and 3-d-simulation of sea-level rise, P.h.D thesis, Ghent University, Ghent, Belgium.

Vandenbohede, A., and L. Lebbe (2007), Effects of tides on a sloping shore: Groundwater dynamics and propagation of the tidal wave, *Hydrogeology Journal*, *15*, 645–658, doi: 10.1007/s10040-006-0128-y.

Veerman, C. (2008), Working together with water; a living land builds for its future, *Report*, Delta Committee.

Vernes, R., and T. H. M. van Doorn (2005), Regis II: Hydrological model of the Neterlands, *Report NITG 05-038-B*, TNO, available at: www.dinoloket.nl.

Visser, M. (2012), Aquifer storage and recovery in a fossil creek bed, M.S.c thesis, University Utrecht, Utrecht.

Vos, P., and F. Zeiler (2008), Holocene transgressions of soutwestern Neterlands, interaction between natural and anthropogenic sources, *Grondboor & Hamer*.

Zagwijn, W. (1974), The paleographic evolution of the Netherlands during the Quatenary, *Geologie an Mijnbouw*, *53*, 369–385.

Zagwijn, W. (1989), The neterlands during the Tertiary and the Quaternary: a case history of coastal lowland evolution, *Geologie an Mijnbouw*, *68*, 107–120.